Latvijas Universitātes Cietvielu Fizikas Institūts

**Mag. Vadims Ogorodņiks**

PROMOCIJAS DARBS

# RADIĀCIJAS DEFEKTU PĒTĪJUMI AR EPR METODI $LiBaF_3$ KRISTĀLĀ



Rīga, 2004

Saturs

Ievads

$LiBaF_3$ kristāls ir perspektīvs pielietojumiem kā materiāls siltuma neitronu detektoriem, kā arī jonizējošā starojuma atmiņas ekrānu materiāls (skat. piem. [1]). $LiBaF_3$ kristālam ir t.s. antiperovskita struktūra un viņu ir salīdzinoši viegli aktivēt ar dažādiem piejaukuma joniem.

Pašreizējā laika posmā šī materiāla īpašības, kā arī konkrētie pielietojumu aspekti atrodas pētījumu stadijā, arī EPR spektru pētījumi $LiBaF_3$ kristālos vēl atrodas sākuma stadijā.

Pirms mūsu darba literatūrā bija publicēti EPR dati tikai par vairākiem pārejas elementu piejaukuma joniem $LiBaF_3$ kristālos, bet radiācijas defektu struktūras pētījumi ar EPR metodi nebija aprakstīti. Tādejādi trūka būtiska informācija par radiācijas defektu struktūru $LiBaF_3$, kas bija nepieciešama, lai labāk izprastu $LiBaF_3$ kristālos notiekošos procesus.

Promocijas darba mērķis bija izpētīt dažus no $LiBaF_3$ kristālu EPR spektriem, kuri rodas rentgenstarojuma rezultātā.

Promocijas darba konkrētie uzdevumi bija:

1) izpētīt LNT apstarotu $LiBaF_3$ kristālu EPR spektrus,
2) izpētīt istabas temperatūrā apstarotu $LiBaF_3$ kristālu EPR spektrus.

Mūsu darbā izpētīti dažādās temperatūrās apstarotu $LiBaF_3$ kristālu EPR spektri un identificēti diviem no radiācijas defektiem- autolokalizētam cauruma centram, jeb $V_K$ centram, kā arī F-tipa centram, atbilstošie EPR spektri un noteikti to parametri.

Promocijas darba rezultāti publicēti 5 zinātniskajās publikācijās (literatūras sarakstā promocijas darba autora publikācijs apzīmētas ar zvaigznīti [2*-6*]), kā arī referēti starptautiskajās konferencēs ICDIM'2000, LUMDETR'2000, EURODIM'2002, LUMDETR'2003.

## 2. Literatūras apskats

Literatūrā ir publicēti EPR pētījumu rezulāti par dažiem $3d^n$ - parejas metālu grupas piejaukumu joniem [7] : $Ti^{3+}$ ($4f^1$) , $Cr^{3+}$ ($3d^3$) , $Mn^{2+}$ ($3d^5$) , $Fe^{3+}$ ($3d^5$) un $Co^{2+}$ ($3d^7$) , kā arī retzemju metālu piejaukuma joniem $Ce^{3+}$ ($4f^1$) [8] .

Noteikti sekojuši spin-hamiltoniāna parametri $d^n$ - pārejas grupas piejaukumu joniem $LiBaF_3$ [7] :

$Ti^{3+}$ ($3d^1$) : $g_{\parallel} = 1.9567$ ; $g_{\perp} = 1.9702$

$Cr^{3+}$ ($3d^3$) : $g = 1.9784$

$Mn^{2+}$ ($3d^5$) : $g = 2.0014$ ; $A = 88.3 * 10^{-4}$ $cm^{-1}$ ; $a = 5.5*10^{-4}$ $cm^{-1}$

$Fe^{3+}$ ($3d^5$) : $g = 2.0025$ ; $a = 120*10^{-4}$ $cm^{-1}$

$Co^{2+}$ ($3d^7$) : $g = 4.3164$ ; $A = 94.7*10^{-4}$ $cm^{-1}$

Šeit g ir g tenzora parametri, A un a attiecīgi hipersīkstruktūras un kristāliskā lauka mijiedarbības raksturojošie spin-hamiltoniāna:

$$H=g\beta\mathbf{S}\bullet\mathbf{B}+A\mathbf{S}\bullet\mathbf{I}+a/6(S_x^4+S_y^4+S_z^4-707/16)$$

parametri.

g - Landē faktors, β - Bora magnetons, **S** - spina operators,

**B** - magnētiskā lauka intensitāte, **I** - kodolu spina operators,

A - hipersīkstruktūras konstante, a - kristāliskā lauka mijiedarbības konstante.

Darbā [8] noteikts, kā $Ce^{3+}$ piejaukuma jons $LiBaF_3$ kristālā iebūvējās ar lādiņu kompensējošām vakancēm. Pēc EPR datiem [8] novērojams tetragonālas simetrijas $Ce^{3+}$ centrs, perturbēts [001] ass virzienā un divi ortorombiski $Ce^{3+}$ centri, kuri perturbēti [110] ass virzienā.

$LiBaF_3$ kristāls ticis pētīts arī ar optiskajām (absorbcija, luminescence), kā arī ar termoluminescentajām metodēm. Literatūrā publicēti dati par ar Ce [9-14] , Mg [15] , $Eu^{2+}$ [9,16,17] , Ni [18,19] , piejaukumu joniem

aktivētiem $LiBaF_3$ kristāliem [20]. Ar optiskajām metodēm pētīti arī F tipa centri $LiBaF_3$ kristālos [21,22].

Termostimulētās luminiscences (TSL) pētījumos novērots termostimulētās luminiscences maksimums ap 139 K, kurš saistīts ar $V_K$ centru termisko sabrukšanu [2*]. Novēroti termostimulētās relaksācijas procesi temperatūru rajonā no 290 - 650 K [23,24], kuri saistīti ar F- tipa centriem. $LiBaF_3$ kristālu pētījumos ar magnetooptiskajām metodēm [25] (magnētiskais cirkulārais dihroisms MCD un optiski detektētais EPR) novēroti MCD spektri, kuri saistīti ar F- tipa centriem, kā arī gūts tiešs apstiprinājums tam, ka $V_K$ centri piedalās zemo temperatūru rekombinatīvajā luminiscencē (tuneļluminiscencē).

## 2.1. $LiBaF_3$ kristāla struktūra

$LiBaF_3$ kristālam ir kubiska, antiperovskīta struktūra ( Zīm 1.). Kristālam ir joniska struktūra ar diviem katjoniem $Li^+$ un $Ba^{2+}$ un 3 anjoniem $F^-$ . Struktūra pieder pie t.s. bezparametriskajām un visu jonu stāvoklis pilnībā var tikt uzdots ar vienu kubiskā režģa parametru. $LiBaF_3$ kristālam režģa parametrs $a_0$ = 3.99 Å . Elementārā šūna satur vienu $LiBaF_3$ formulas vienību.

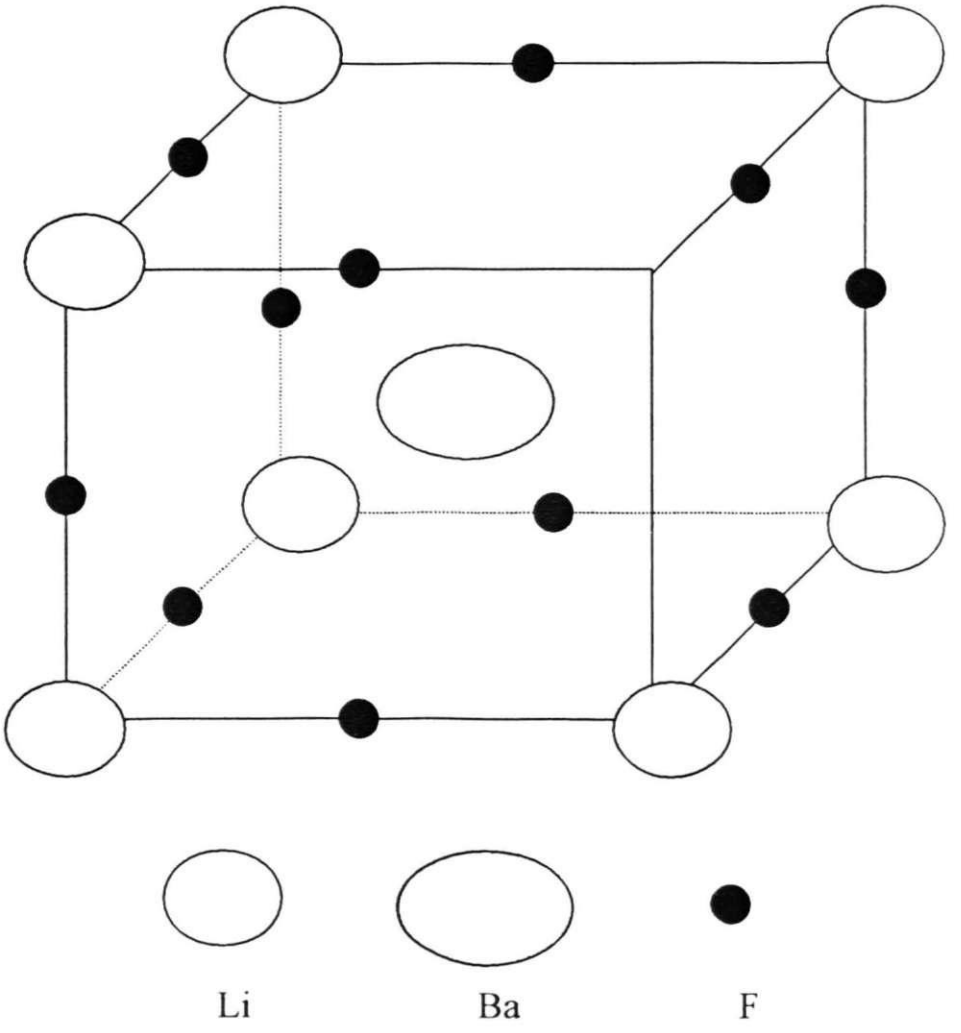


Zīm.1. $LiBaF_3$ kristāla struktūra.

2.2 EPR metodes pamatprincipi.

Elektronu paramagnētiskā resonanse (EPR) – rezonanses elektromagnētiskās enerģijas absorbcija vielā, kura satur paramagnētiskas daļiņas. Izplatītākais elektromagnētiskā starojuma avots ir t.s. klistrons (elektronu lampa, kura ģenerē superaugsto frekvenču (SAF) diapazonā). Paramagnētiskai vielai, kura atrodās magnētiskajā laukā, spinu līmeņi sašķeļās, enerģiju starpība starp sašķeltajiem apakšlīmeņiem ir gβH. Ja SAF kvanta enerģija hν sakrīt ar enerģiju starpību starp sašķeltajiem apakšlīmeņiem hν = gβH, notiek SAF kvanta rezonanses absorbcija un elektrons pāriet no zemākā apakšlīmeņa uz augstāko. EPR metodi izmanto, lai izpētītu paramagnētiskus jonus, kā arī elektronu un caurumu ķerājcentrus vielā jebkurā tās agregātstāvoklī (cietā, šķidrā, kā arī gāzveida). Piejaukuma centri cietā vielā rada paramagnētiskos jonus ar daļēji aizpildītām čaulām. Nesapārotais spins rada visa jona magnētisko momentu, kurš var būt atšķirīgs no nulles. Visbiežāk sastopamas neaizpildītas d- un f- čaulas (s- un p- čaulas parasti piedalās ķīmiskās saites veidošanā kristālā un veido elektronu konfigurācijas ar sapārotiem spiniem un nulles magnētisko momentu). Arī elektronu un caurumu ķērājcentrus var pētīt ar EPR metodi, jo elektrona vai cauruma saķeršana uz defekta var pārveidot defektu paramagnētiskā stāvoklī. EPR metode var sniegt informāciju par defektu centru ģeometrisko, kā arī elektronisko struktūru.

Elektronu un caurumu centrus kristālā var radīt arī ar starojumu (rentgena, gamma, alfa, beta, neitronu u. tml.) palīdzību, šādus centrus sauc par radiācijas defektiem [26].

Pēc būtības, izpētīt defektu analīze ar EPR metodi nozīmē veikt rezonanses absorbcijas spektru analīzi. Spektrs tiek analizēts pēc sekojošiem krītērijiem: līniju skaita, to intensitātēm, savstarpējā novietojuma, kā arī EPR spektra līniju leņķiskajām atkarībām [27,28].

EPR spektros novērojamās līnijas iedala, vadoties pēc mijiedarbībām, kuras nosaka enerģijas līmeņu sašķelšanos:

1) elektronu Zēmana efekts,
2) spektra sīkstruktūra (kuru nosaka enerģijas līmeņu sākotnējā sašķelšanās kristāliskajā (elektriskajā) laukā),
3) spektru hipersīkstruktūra (kuru nosaka nesapārotā spina mijiedarbība ar kodolu spinu magnētiskajiem momentiem).

Zēmana efektā t.s. Zēmana apakšlīmeņu skaits ir 2S+1, izvēles likums atļautajām EPR pārejām: $\Delta M_S = \pm 1$, kā rezultātā atļauto pāreju skaits ir 2S. Spektru hipersīkstruktūras līniju skaitu nosaka kodola spins I. Izvēles likumi atļautajām pārejām : $\Delta M_S = \pm 1$; $\Delta M_I = \pm 0$, atļauto pāreju skaits ir $2I + 1$.

EPR spektru simetrija un leņķiskās atkarības dod informāciju par defektā ietilpstošā nesapārotā spina galvenajām mijiedarbībām un mijiedarbības tensoru asu orientāciju kristālā.

Vispārīgo EPR spektra aprakstu var iegūt, izmantojot t.s. spin-Hamiltoniāna operatoru: $H = b_e^m O_e^m + g\beta B + \Sigma SAI$

Pirmais loceklis apraksta līmeņu sākotnējo sašķelšanos kristāliskajā laukā, otrais loceklis apraksta Zēmana sašķelšanos, bet trešais loceklis apraksta hipersīkstruktūras sašķelšanos. Visas trīs aplūkotās galvenās mijiedarbības vispārīgajā gadījuma ir aprakstāmas ar t.s. mijiedarbības tenzoru. Atsevišķos gadījumos mijiedarbības iespējams aprakstīt ar skalāriem lielumiem (g, A), vai arī defektam ir aksiāla simetrija un attiecīgie mijiedarbību raksturojoši parametri tādā gadījumā ir: $g_\perp$, $g_{||}$ un $A_\perp$, $A_{||}$.

## 3. Paraugi un eksperimentu metodika

Visi dotajā darbā pētītie paraugi izaudzēti LU cietvielu fizikas institūtā kristāluaudzēšanas laboratorijā (Ā. Veispāls) ar Čohraļska un Stokbargera metodēm. Pētīti gan nomināli tīri $LiBaF_3$ kristāli, gan arī ar Fe, Ni un citiem piejaukumiem. Vairākuma izaudzētie paraugi bija polikristāliski, ar mozaīkveida blokiem, tikai ļoti nedaudzi no audzētajiem kristāli izrādījās monokristāliski. Tādēļ EPR spektru leņķisko atkarību mērījumiem bija no liela daudzuma paraugiem ar rentgenstruktūranalīzes medodi (I. Brante, V. Ogorodņiks) jāatlasa monokristāliskie paraugi.

$V_K$ centru EPR spektru leņķiskās atkarības tika izmērītas nomināli tīrā monokristāliskā paraugā, kurš tika orientēts LU Fizikas un matemātikas fakultātes rentgenstrukturanalīzes laboratorijā. F-tipa centri EPR spektru leņķiskās atkarības tika mērītas $LiBaF_3$ paraugā ar Fe piejaukumu, kurš tika orientēts ar renggenstruktūranalīzas metodēm Čehijas ZA 2. Fizikas institūtā Pragā. Radiācijas defektu radīšanai paraugos tika izmantots rentgenstarojums, paraugus apstarojot gan istabas temperatūrā, gan šķidrā slāpekļa temperatūrā. Tika izmantota rentgeniekārta УРС –55 ar pielikto spriegumu 55 kV, anodstrāva 10 mA, rentgenlampas anods no volframa. apstarošanas laiks 30-60 min. Paraugi gan apstarošanas, gan EPR mērījumu laikā tika turēti tumsā, lai novērstu pētīto defektu sabrukšanu gaismas iespaidā. Paraugu apstarošanai rentgenstarojumu šķidrā slāpekļa temperatūrā tika izmantots stikla djuārs. Paraugs pēc apstarošanas kopā ar škidro slāpekli tika pārvietots EPR spektrometrā kvarca djuārā un mērījumi šajā gadijumā arī tika veikti škidrā slāpekļa temperatūrā (77 K).

EPR spektri tika mērīti ar radiospektrometru РЭ –1306, magnetiskā lauka indukcijas merīšanai tika izmantots Holla devejs (ar voltmetru B7-34A). Mērāmais EPR signāls ar voltmetru B7-23 (pirmais atvasinājums no

kristāla absorbētā SAF starojuma) kopā ar Holla devēja spriegumu tika ievadīti datora faila veidā.

EPR spektru leņķisko atkarību mērījumi tika veikti, griežot paraugu ap vertikālu asi ar 5° soli, kā parādīts eksperimenta shēmā zīmējumā 2.

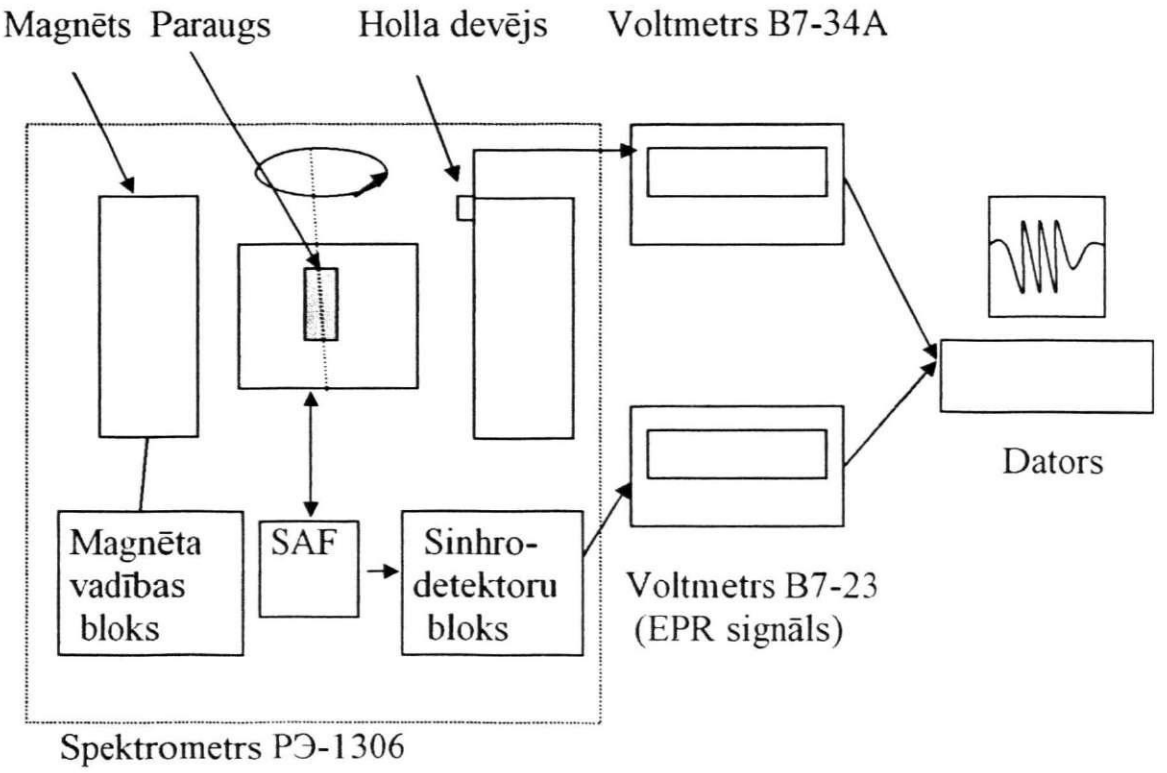


Zīm. 2. EPR eksperimentu shēma.

Darbā EPR spektru teorētiskajam aprēķinam tika izmantotas divas $V_K$ centru EPR spektru leņķiskās atkarības tika izmērītas nomināli tīrā monokristāliskā paraugā, kurš tika orientēts LU Fizikas un matemātikas fakultātes rentgenstrukturanalīzes laboratorijā. F-tipa centri EPR spektru leņķiskās atkarības tika mērītas $LiBaF_3$ paraugā ar Fe piejaukumu, kurš tika orientēts ar renggenstruktūranalīzas metodēm Čehijas ZA 2. Fizikas institūtā Pragā. Radiācijas defektu radīšanai paraugos tika izmantots rentgenstarojums, paraugus apstarojot gan istabas temperatūrā, gan šķidrā slāpekļa temperatūrā. Tika izmantota rentgeniekārta УРС –55 ar pielikto spriegumu 55 kV, anodstrāva 10 mA, rentgenlampas anods no volframa, apstarošanas laiks 30-60 min. Darbā EPR spektru teorētiskajam aprēķinam tika izmantotas divas Paderbornas Universitātē (Vācijā) izstrādātās programmas:

1) HEDOR - $V_K$ centru EPR spektru aprēķinam,

2) PCS - F-tipa centru EPR spektru aprēķinam.

Programma HEDOR atļāva korekti aprēķināt $V_K$ centru EPR spektru leņķiskās atkarības, ievērojot nesapārotā spina hipersīkstruktūras mijiedarbību ar divu fluora kodolu spiniem.

F-tipa centru EPR spektru hipersīkstruktūras aprēķinā jāņem vērā spina mijiedarbība ar pavisam kopā 10 kodolu spiniem, kā arī g-tenzora anizotropija. Tā kā šādas sarežģītības uzdevumu jebkurai patvaļīgai magnētiskā lauka orientācijai nebija iespējams atrisināt ne ar vienu no pieejamām programmām, uzdevums tika sadalīts daļās un risināts tikai trim magnētiskā lauka orientācijām pret $LiBaF_3$ kristāla galvenajām asīm. Vispirms ar programmu PCS tika aprēķināta spektru hipersīkstruktūra katrai no dotajā orientācijā sastopamajiem g- faktoriem un tad šie spektri

sasummēti. Lai paātrinātu spektru aprēķinu šādā veidā, visu PCS programmā ievadāmo tenzoru komponenšu noteikšanai tika izveidots algoritms Excel tabulas veidā.

## 4. Eksperimentu rezultāti

Radiācijas defektu EPR spektri $LiBaF_3$ kristālos tika pētīti, gan apstarojot paraugus 77 K (LNT), gan istabas temperatūrā (300 K, RT).

LNT apstarotu $LiBaF_3$ kristālu EPR spektrā (zīm.3) redzama intensīva centrālo līniju grupa, kura pieder neidentificētiem defektiem un to mēs mūsu darbā tālāk neaplūkosim. Mūsu darbā mēs analizēsim trīs vājāku līniju grupas, kuras mēs identificējām kā dažādi orientētu $V_K$ centru līnijas (zīm 3, zīm. 4). Šo līniju grupu leņķiskās atkarības mes sīkāk aprakstīsim punktā 4.1. [2*-4*].

RT apstarota $LiBaF_3$ kristāla EPR spektrā (zīm 5) arī redzama intensīva centrālā līnija, kura arī pieder neidentificētiem defektiem, ko mēs tālāk neaplūkosim. Mēs pētīsim EPR līniju grupu, kura sastāv no apmēram 35 līnijām. Šīs grupa EPR līnijas arī stipri mainās no kristāla orientācijas pret magnētisko lauku. Taču, ja līniju novietojumam ir samērā vāja leņķiskā atkarība, tad ļoti izteikta leņķiskā atkarība ir grupas līniju intensitātēm, šīs leņķiskās atkarības mēs sīkāk aplūkosim punktā 4.2. [5*-6*].

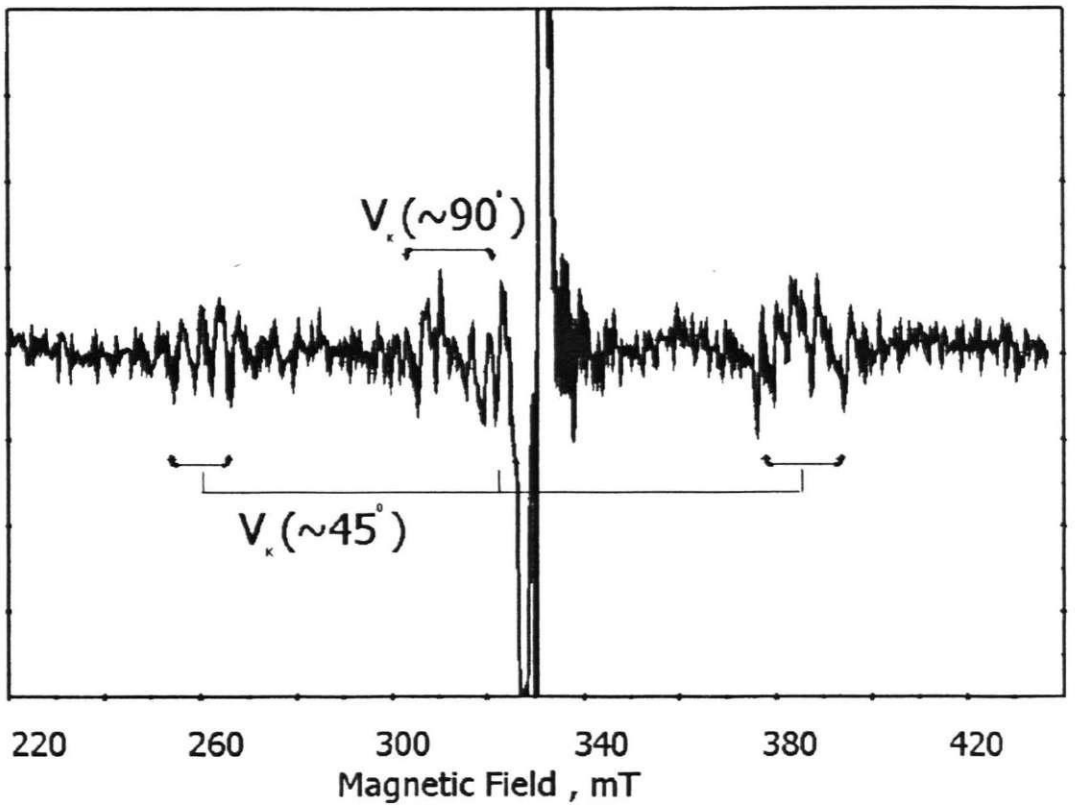


Zīm. 3. LNT apstarota $LiBaF_3$ kristāla EPR spektrs.

4.1. $V_K$ centru EPR spektri $LiBaF_3$ un to leņķiskā atkarība

LNT apstarota $LiBaF_3$ kristāla EPR spektra līniju leņķiskā atkarība parādīta 4. zīmējumā. Eksperimentālā EPR līnijas izvietotas gandrīz simetriski pret magnētiskā lauka vērtībām 320-330 mT. Gan kreisajā, gan labajā spektra pusē var novērot līdz 6 resonanses līnijām. EPR spektrs vienkāršojas pie magnētiskā lauka orientācijas $\mathbf{B}\,||\,[100]$. Šajā magnētiskā lauka orientācijā eksperimentāli novērojamās resonanses līnija saiet kopā 4 grupās – 2 grupās katrā pa 4 līnijām un spektra vidus daļā – 2 grupās pa 2 līnijām. Pašā centrālajā EPR spektra daļā (ap 330 mT), līniju gaitu izsekot traucē intensīvā līnija no neidentificētajiem radiācijas defektiem. 5 nodaļā mēs aplukosīm šo EPR spektru teorētisko modelēšanu.

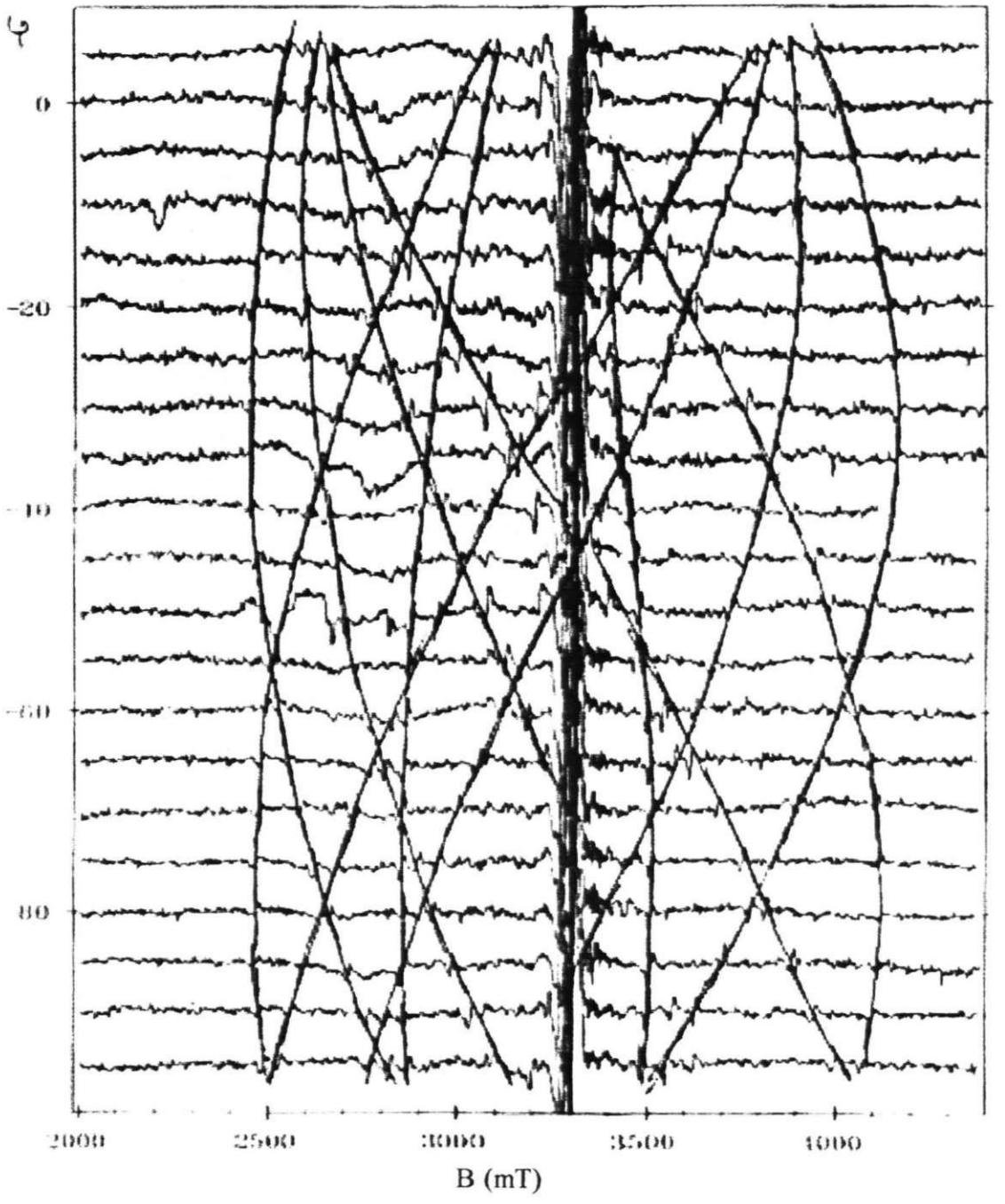


Zīm. 4. LNT apstarotu $LiBaF_3$ kristālu EPR spektri un to leņķiskā atkarība.

## 4.2. F-tipa centru EPR spektri $LiBaF_3$ un to leņķiskā atkarība

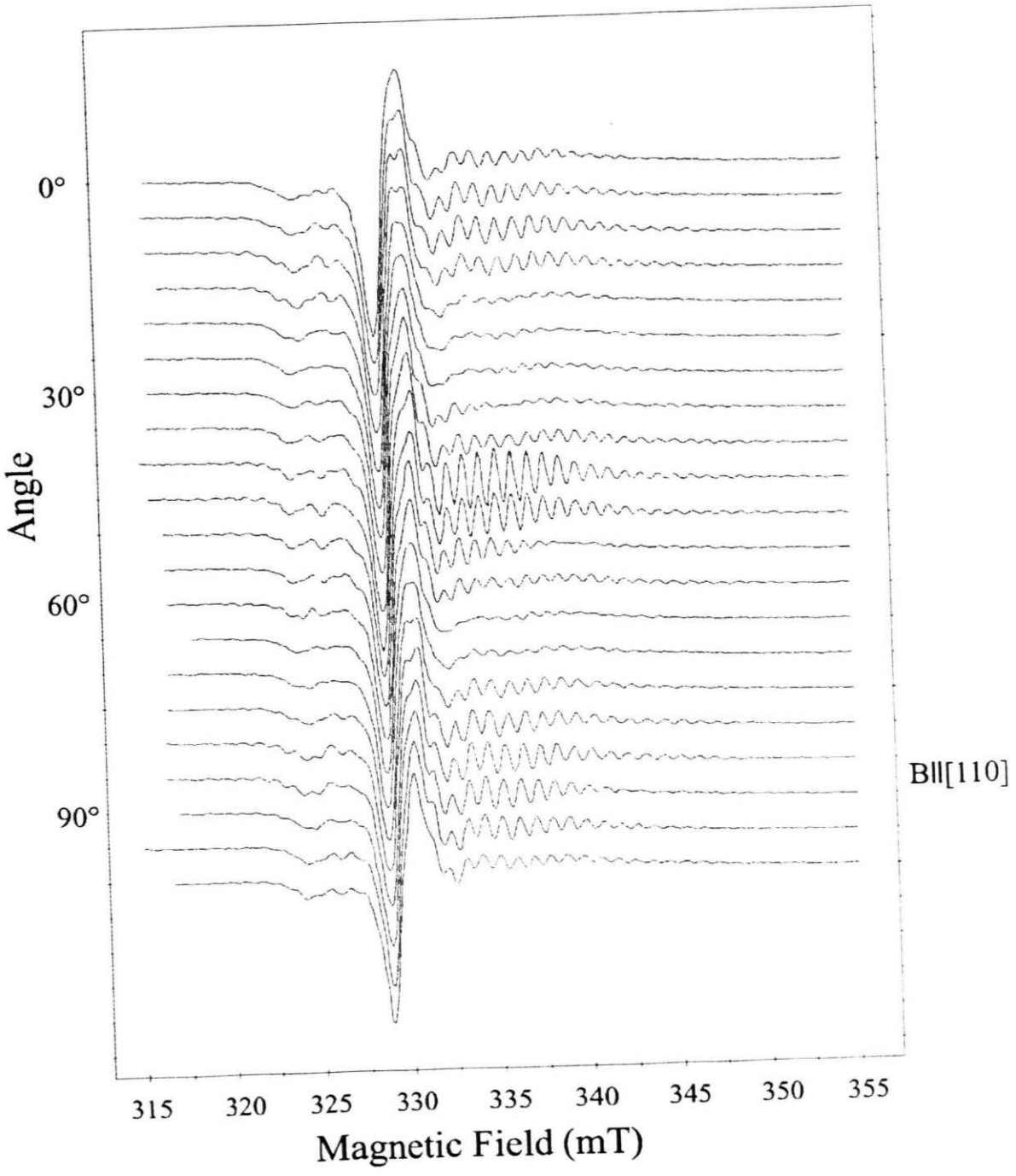


Zīm 5. RT apstarota $LiBaF_3$ kristāla EPR spektri $LiBaF_3$ un to leņķiskā atkarība.

Istabas temperatūrā apstarota $LiBaF_3$ kristāla EPR spektra līniju leņķiskā atkarība parādīta 5. zīmējumā. 35 līniju grupā, mainoties kristāla orientācijai pret magnētiskā lauka virzienu, novērojamas straujas izmaiņas. Tuvāka analīze parādīja, ka atsevišķi līniju novietojums un attālums izmainās relatīvi nedaudz, bet straujās izmaiņa nosaka gan līniju absolūto intensitāšu, gan relatīvo intensitāšu leņķiskā atkarība.

Vislielākā grupas līniju intensitāte novērojama pie magnētiskā lauka orientācijas $\mathbf{B} \| [111]$, šajā orientācijā arī līniju grupa relatīvais intensitāšu sadalījām ir ļoti tuvs binomiālajam.

Līniju intensitāšu leņķiskā atkarība ir ļoti izteikta, dažkārt magnētiskā lauka izmaiņa jau par 5° noved pie pilnīgas, kvalitatīvas grupas līniju intensitāšu relatīvās izmaiņas. Dažās orientācijas 35 līniju grupa sadalās vairākās apakšgrupās ar ļoti dažādām amplitūdām.

Šīs EPR līniju grupas līniju skaits un to leņķiskās atkarības $LiBaF_3$ mūsu darbā izskaidrota F-tipa centra modeļa ietvaros un to teorētiskā modelēšana aplūkota 6. nodaļā.

## 5. $V_K$ centru EPR spektru modelēšana

No novērotajām LNT apstarotā $LiBaF_3$ kristāla, EPR spektru leņķiskajām atkarībām mēs varam secināt, ka EPR spektru nosaka 6 magnētiski ekvivalenti centri. Hipersīkstruktūras mijiedarbības tenzoru galvenās asis vērstas [110] virzienā. Nesapārotā spina vērtība S=1/2 un līniju un to grupu skaitu var izskaidrot ar hipersīkstruktūras mijiedarbību ar 2 fluora $^{19}F$ kodolu spiniem (I=1/2, izotopa dabiskais saturs – 100%) katrā centrā. Šāds modelis atbilst $V_K$ centram $LiBaF_3$ kristālā.

$V_K$ centrs ir autolokalizēts cauruma centrs, kurā caurums lokalizēts uz diviem fluora anjoniem un tā ass virzīta kristalogrāfiskajā virzienā <110>. Vienkāršoti šo defektu var stādīties priekšā kā $F_2^-$ jonu.

## 5.1. Spektru anizotropija

Zīmējuma 6 parādīta $V_K$ centram, ar tā galveno asi virzītu [110] virzienā, atbilstošo EPR līniju kvalītatīvi leņķiskā atkarība, ja magnētiskā lauka indukcijas virziens mainās kristāla (100) plaknē.

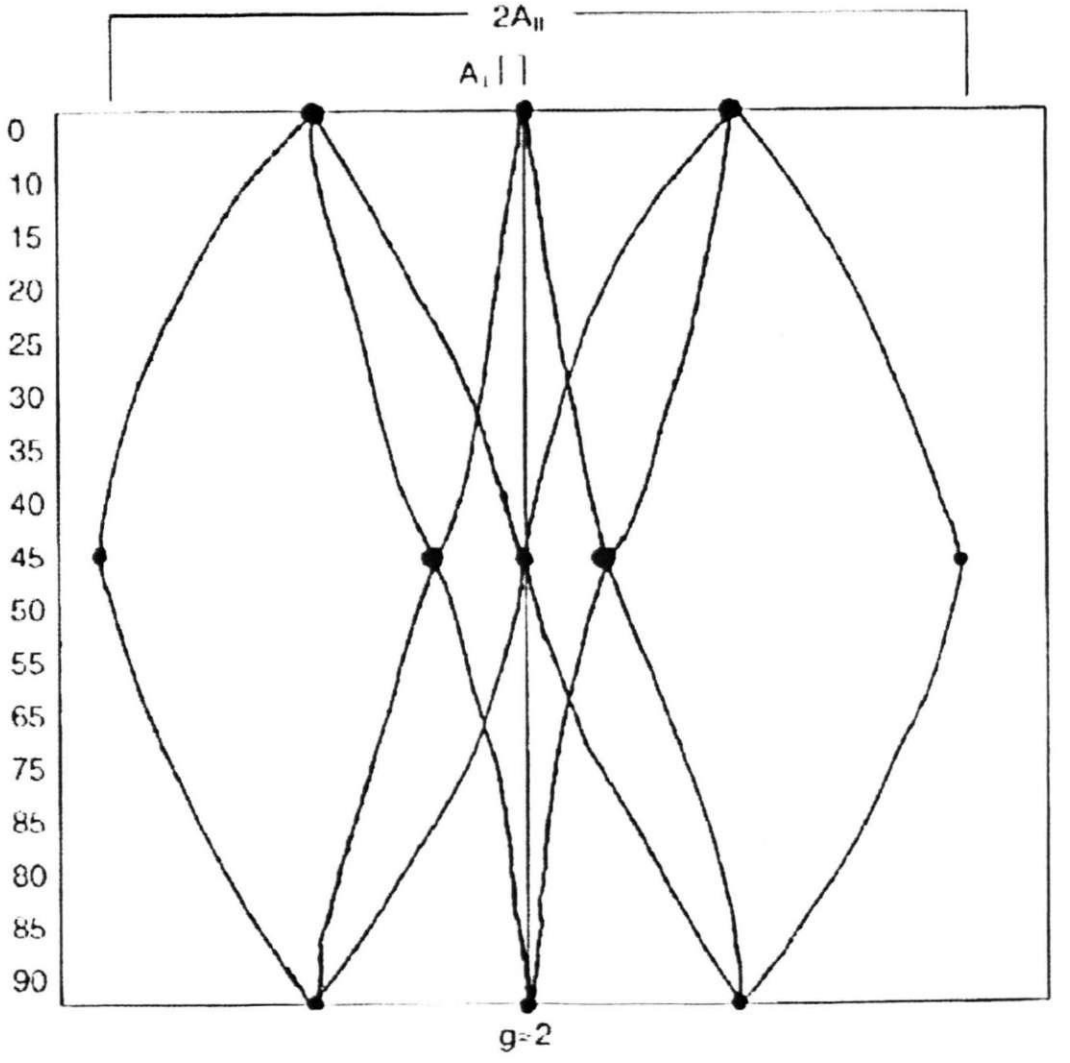


Zīm. 6. Kvalitatīvs $V_K$ centra EPR spektra izskats

5.2. Centra modelis un spin-Hamiltoniānis

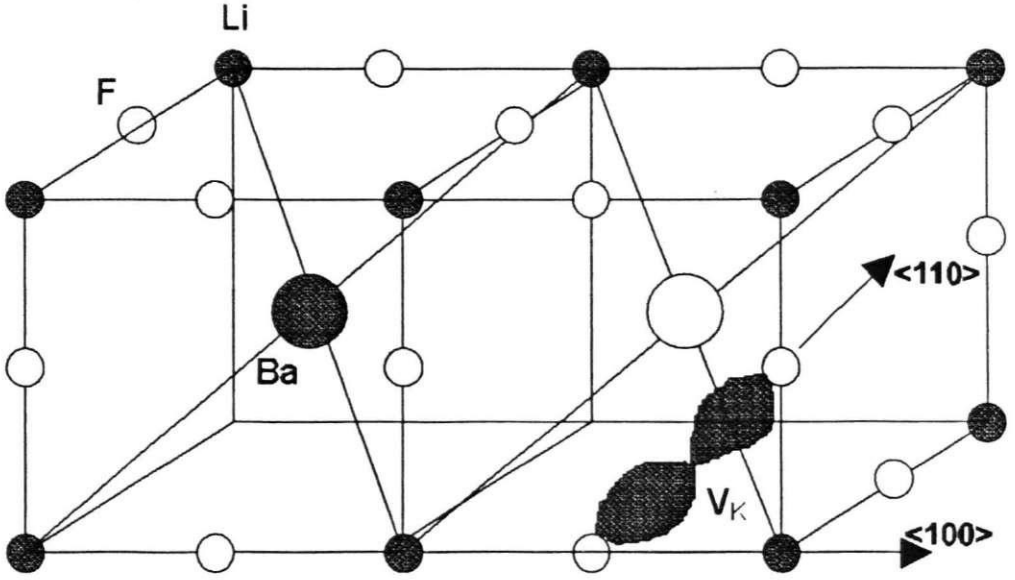


Zīm. 7. $V_K$ centra modelis $LiBaF_3$ kristālā. $V_K$ centra modelis parādīts 7.

zīmējumā, EPR spektru aprēķinam izmantots spin-Hamiltoniānis:

$$H=g\beta SB+2*SA_FI_F \quad (1),$$

Kur g ir g-tenzors, β - Bora magnetons, $A_F$ – hipersīkstruktūras mijiedarbības tenzors,

Nesapārotais spins S=1/2 un fluora kodolu spins $I_F=1/2$.

Hipersīkstruktūras tenzors $V_K$ centra gadījumā ir ar aksiālu simetriju:

$$\mathbf{A} = \begin{pmatrix} A_\perp & 0 & 0 \\ 0 & A_\perp & 0 \\ 0 & 0 & A_{||} \end{pmatrix}$$

Tabula 1 uzdoti mūsu aprēķinu resultātā iegūtie $V_K$ centra g-tenzora un hipersīkstruktūras tenzora parametri $LiBaF_3$ kristālā.

Tabula 1. $V_K$ centra $LiBaF_3$ kristālā spin-Hamiltoniāna parametri.

| $A_{\|}$ =2520±20 (MHz) | $A_\perp$=200±30 (MHz) | $g_{\|}$= 2.002±0.002 | $g_\perp$=2.024±0.002 |
|---|---|---|---|

5.3. Teorētiski aprēķinātie $V_K$ centru EPR spektri.

Izmantot spin-Hamiltoniāni (1) un 1. tabulā uzdotos $V_K$ centra EPR parametrus, aprēķinātais $V_K$ centra EPR spektrs parādīts zīmējumā 8.

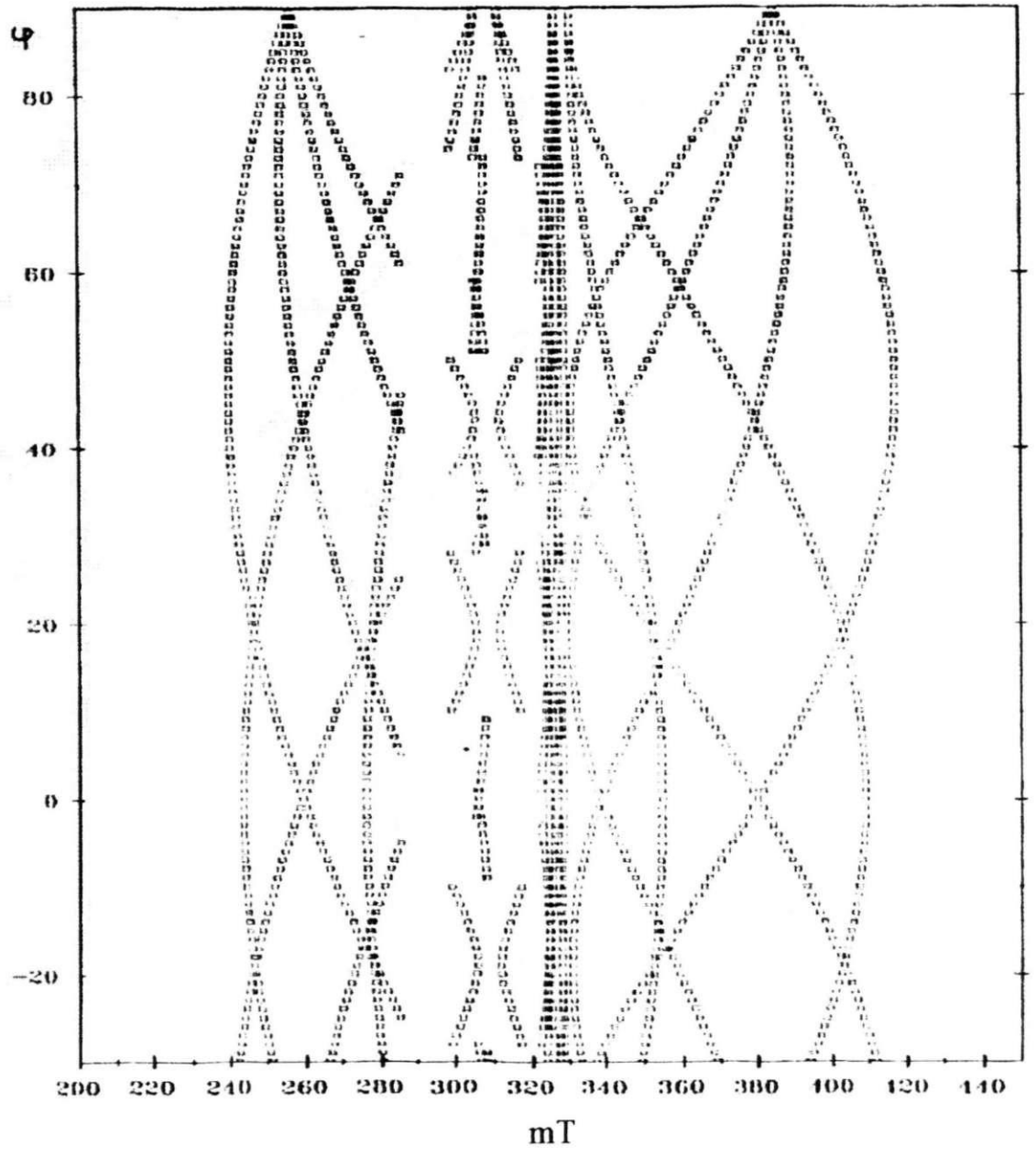


Zīm 8. $V_K$ centra teorētiskie EPR spektri $LiBaF_3$ kristālā.

Zīmējumā 9 teorētiskais $V_K$ centra EPR spektrs apvienots ar eksperimentālā EPR spektra punktiem (kuri attēloti ar kvadrātiņiem). Labā teorētisko un eksperimentālo datu sakritība apliecina mūsu izvēlētā defekta modeļa - $V_K$ centrs $LiBaF_3$ kristālā - pareizību.

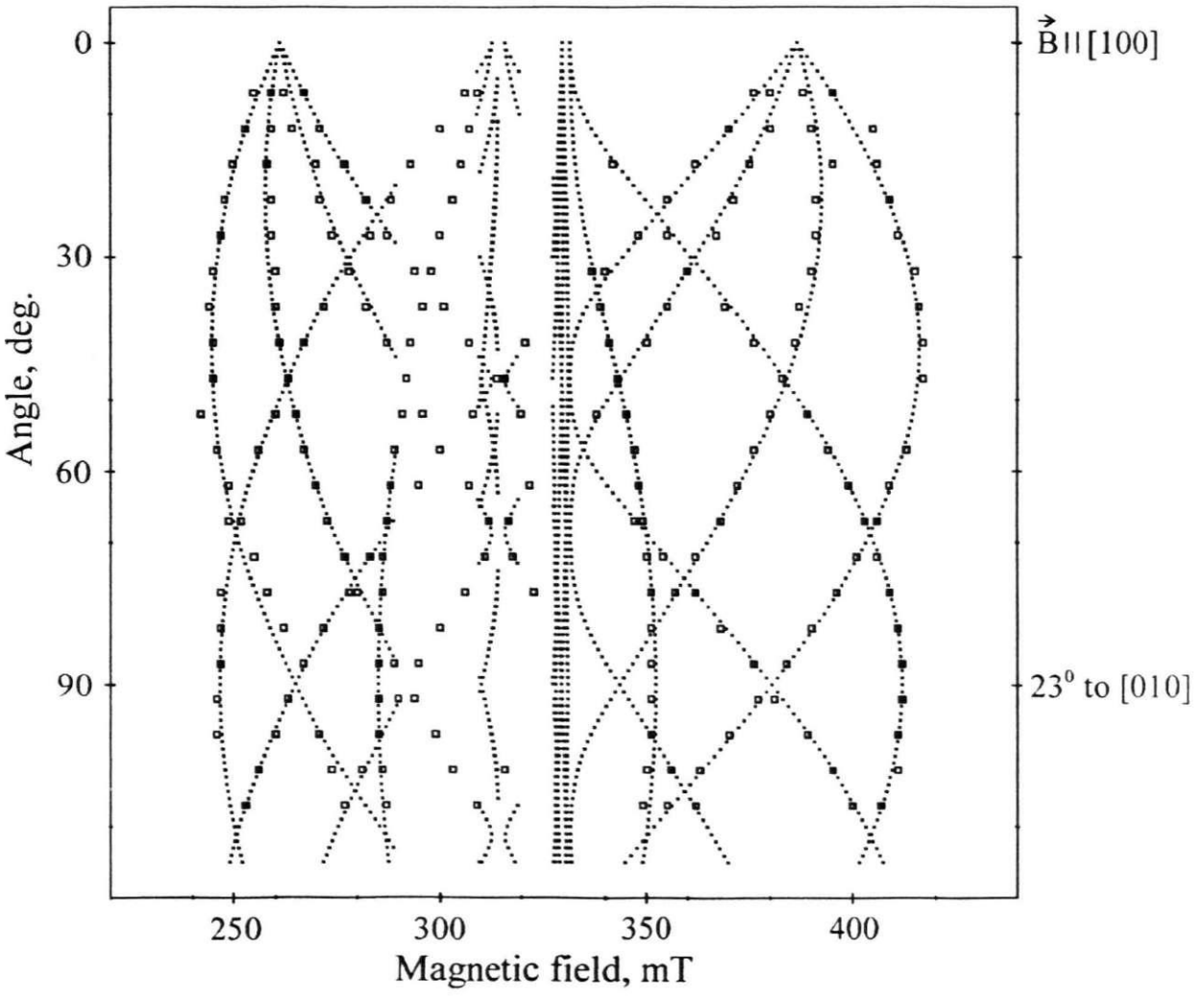


Zim 9. EPR spektrs $V_K$ teorētiskais un eksperimentālie spektri (leņķiskā atkarība). Spektrs mētīts 77 K temperatūrā, mikroviļņu frekvence 9.18 GHz.

## 5.4. Secinājumi

LNT apstarotajā $LiBaF_3$ kristālā novērotā defekta eksperimentālo EPR spektru un tā leņķiskās atkarības labi izdodas aprakstīt ar $V_K$ centra teorētisko modeli – caurumu, kurš autolokalizējies un diviem fluora anjoniem ar molekulas asi virzītu <110> virzienā.

## 6. F-tipa centru EPR spektru modelēšana

Istabas temperatūrās apstarotā $LiBaF_3$ kristālā novērotā EPR līniju grupu, sastāvošu no apmēram 35 līnijām, neizdevās ilgāku laiku izskaidrot līniju intensitāšu straujo leņķisko atkarību dēļ. Atrisinājumam izdevās pietuvoties tikai pēc tam, kad tika atrasta eksperimentālo spektru kvalitatīva analoģija ar literatūrā atrodamo F centra EPR LiF kristālā [29]. Kaut gan LiF kristālā F centra nesapārotajam elektronam ir atšķirīgs kaimiņu kodolu skaits, mums izdevās dotajam $LiBaF_3$ uzdevumam izmantot darbā [29] uzdotos hipersīkstruktūras mijiedarbības parametrus Li un F kodoliem.

Mūsu darbā izvirzītajā F-tipa centra modelī $LiBaF_3$ kristālā nesapārotais elektrons ar S=1/2 mijiedarbojās ar lielu skaitu kaimiņiem kodolu spiniem: ar 2 Li kodolu spiniem I koordinācijas sfērā (attālums a/2) un 8 F kodolu spiniem II koordinācijas sfērā (attālums $a\sqrt{2}/2$).

6.1. Spektru anizotropija

Zīmējumā 10. parādīti istabas temperatūrā apstarota $LiBaF_3$ kristāla EPR spektri, ja magnētiskais lauks orientēts kristāla galveno asu virzienos. Pats intensīvākais EPR spektrs magnētisko lauku rajonā 335÷355 mT novērojams, kad B || [111], spektrs kopumā satur apmēram 35 ekvidistantas līnijas. Orientācijā B || [110] EPR spektrā var labi novērot minētās līniju grupas sadalīšana divās grupās. Trešajā orientacijā, kad B || [100], visu līniju amplitūda apskatāmajā EPR spektrā no 335÷355 mT ir stipri samazinājusies.

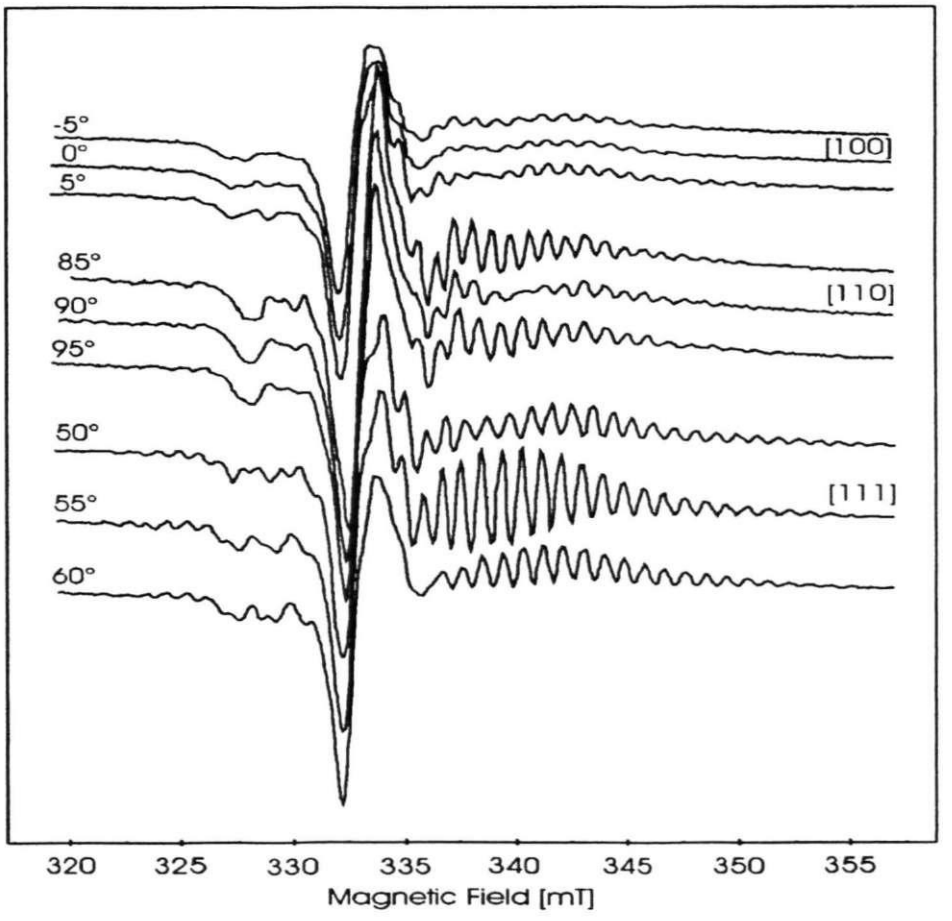


Zīm. 10. RT apstarota $LiBaF_3$ kristāla EPR spektri galveno asu virzienos. Mikroviļņu frekvence (9.37, 9.38, 9.38 GHz).

6.2. Centra modelis un spin-Hamiltoniānis

11. Zīmējumā attēlots F-tipa centra modelis $LiBaF_3$ kristālā. Parādīta fluora vakance un tā tuvākie kaimiņi – 2 Li joni (I) un tālākajā (II) koordinācijas sfērā – 8 fluora joni.

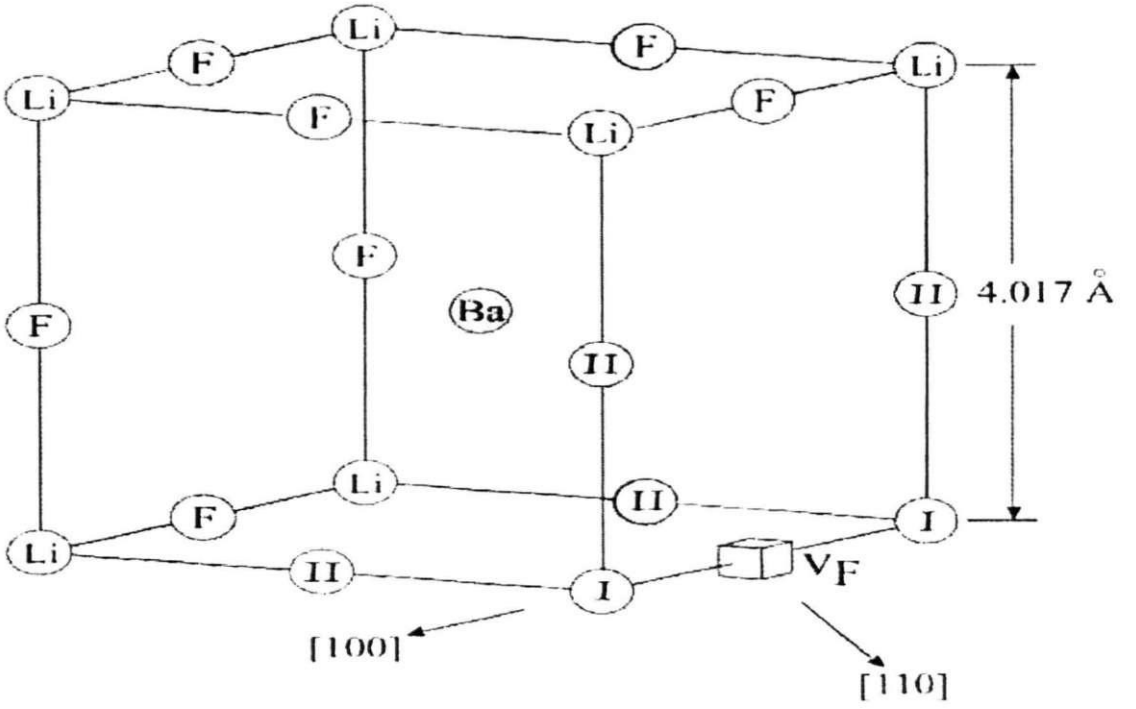


Zīm. 11. F-tipa centra modelis $LiBaF_3$ kristālā.

F-tipa centra EPR spektru aprakstam izmantotais spin-Hamiltoniānis:

$$H=g\beta SB+8*SA_FI_F+2*SA_{Li}I_{Li} \quad (2),$$

kur hipersīkstruktūras mijiedarbības tenzors:

$A_\perp=a-b$

$A_{||}=a+2b$

$$A=\begin{pmatrix} A_\perp & 0 & 0 \\ 0 & A_\perp & 0 \\ 0 & 0 & A_{||} \end{pmatrix}$$

Nesapārotā elektrona spins: S=1/2 un hipersīkstruktūras mijiedarbības iesaistīto kodolu spini: $I(Li^6)=1$ (7.5%), $I(Li^7)=3/2$ (92.5%), I(F)=1/2 (100%).

g-tenzora komponentu aprēķinam patvaļīgā leņķī α tika izmantota sakarība:

$g^2(\alpha)=g_{\perp}^2*\sin^2\alpha+ g_{\parallel}^2*\cos^2\alpha$

Hipersīkstruktūras mijiedarbības konstantes aprēķinam patvaļīgā leņķī α:

$$A_\alpha = \sqrt{A_\perp^2 * \sin^2\alpha + A_{||}^2 * \cos^2\alpha}$$

2. Tabulā apkopoti mūsu darbā noteiktie F-tipa centru g-tenzora un hipersīkstruktūras tenzoru parametri.

| a ($F^{19}$) (mT) | b ($F^{19}$) (mT) | a ($Li^7$) (mT) | b ($Li^7$) (mT) | $g_{\parallel}$ | $g_{\perp}$ |
|---|---|---|---|---|---|
| 3.12 | 0.20 | 0.91 | 0.03 | 1.990 | 1.960 |
| ±0.02 | ±0.02 | ±0.02 | ±0.01 | ±0.005 | ±0.005 |

Tabula 2. F-tipa centra g-tenzora un hipersīkstruktūras tenzora parametri.

6.3. Teorētiski apreķinātie F tipa centru EPR spektri

EPR spektru aprēķinam orientācijā B || [111], izmantojot tabulā 2. dotos spin-Hamiltoniāna parametrus, tika atsevišķi izrēķinātas atbilstošās g-tenzora un visu hipersīkstruktūras tenzoru komponenšu vērtības.

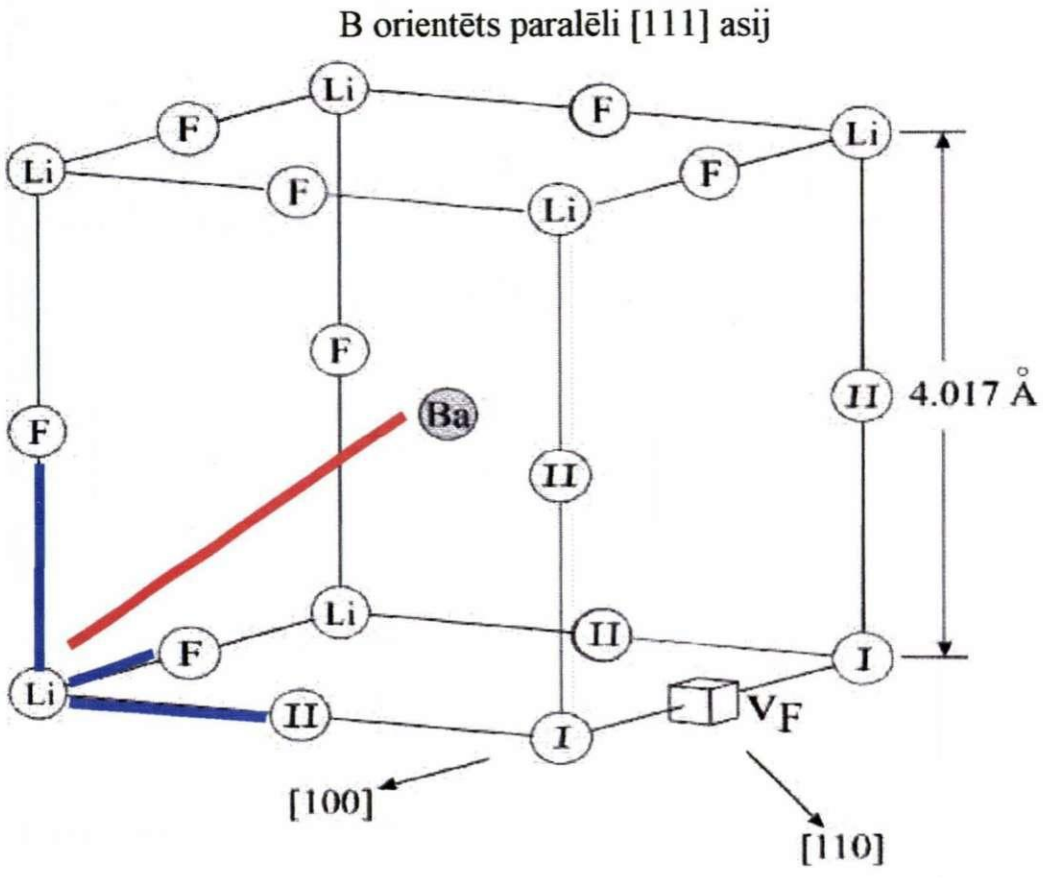


Zīm. 12. F-tipa centra EPR spektra aprēķini <111> virzienā: g-tenzora un hipersīkstruktūras tenzora parametru vērtības dažādām centru orientācijām X, Y, Z (φ=54°)

$g_{54}$= 1,967 ± 0.005

4 F = 75,53 MHz

4 F = 99,22 MHz

2 Li = 25,14 MHz

13. Zīmējumā aprēķinātie EPR spektri F-tipa centram orientācijā B||[111], salīdzināti ar RT apstarotā $LiBaF_3$ kristāla atbilstošo eksperimentālo EPR spektru.

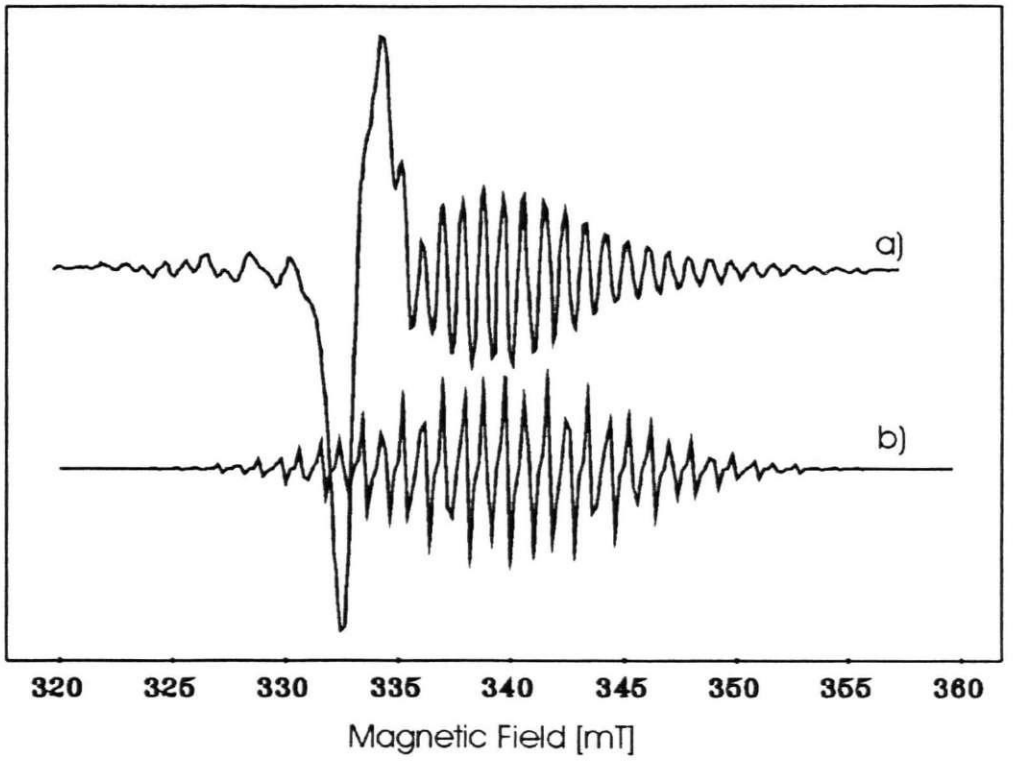


Zīm. 13. F-tipa centra EPR spektri $LiBaF_3$ kristālā
<111> virzienā (eksperimentālie- **a** un teorētiskie- **b**)

EPR spektru aprēķinam orientācijā B || [110], izmantojot tabulā 2. dotos spin-Hamiltoniāna parametrus.

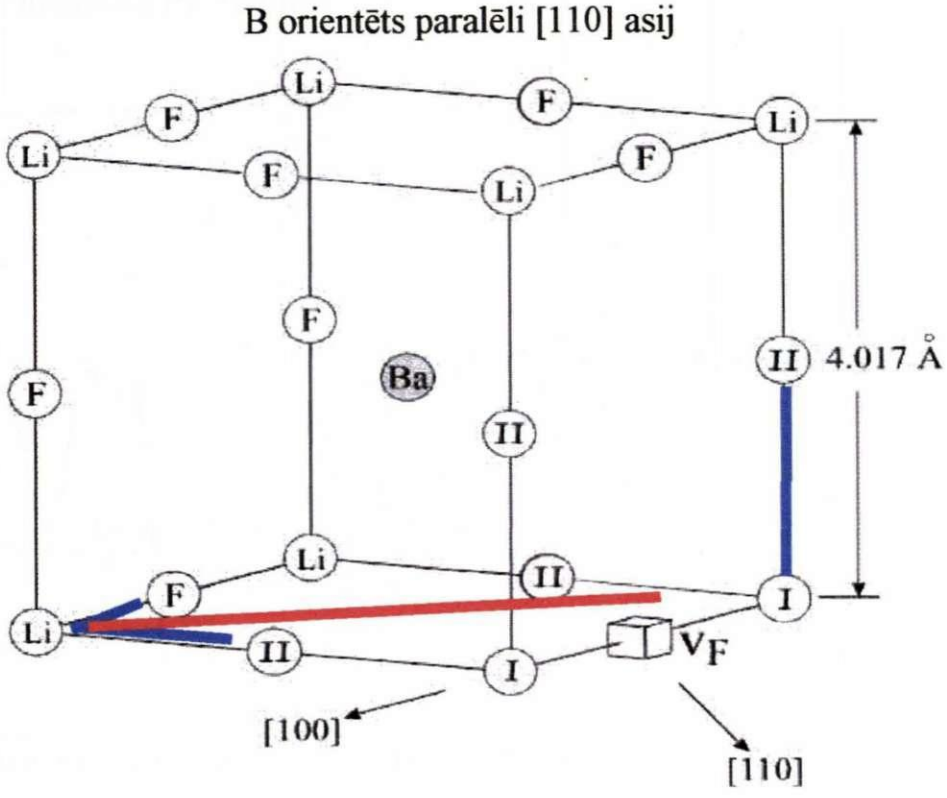


Zīm. 14. F-tipa centra EPR spektra aprēķini <110> virzienā: g-tenzora un hipersīkstruktūras tenzora parametru vērtības dažādām centru orientācijām

| X, Y (φ=45°) | Z (φ=90°) |
|---|---|
| $g_{45}$ = 1,975±0,005 | $g_{\perp}$ = 1,960±0,005 |
| 2 F = 75,67 MHz | 8 F = 86,41 MHz |
| 2 F = 112,66 MHz | 2 Li = 22,98 MHz |
| 4 F = 86,41 MHz | |
| 2 Li = 26,09 MHz | |

15. Zīmējumā aprēķinātie EPR spektri F-tipa centram orientācijā B||[111], salīdzināti ar RT apstarotā $LiBaF_3$ kristāla atbilstošo eksperimentālo EPR spektru.

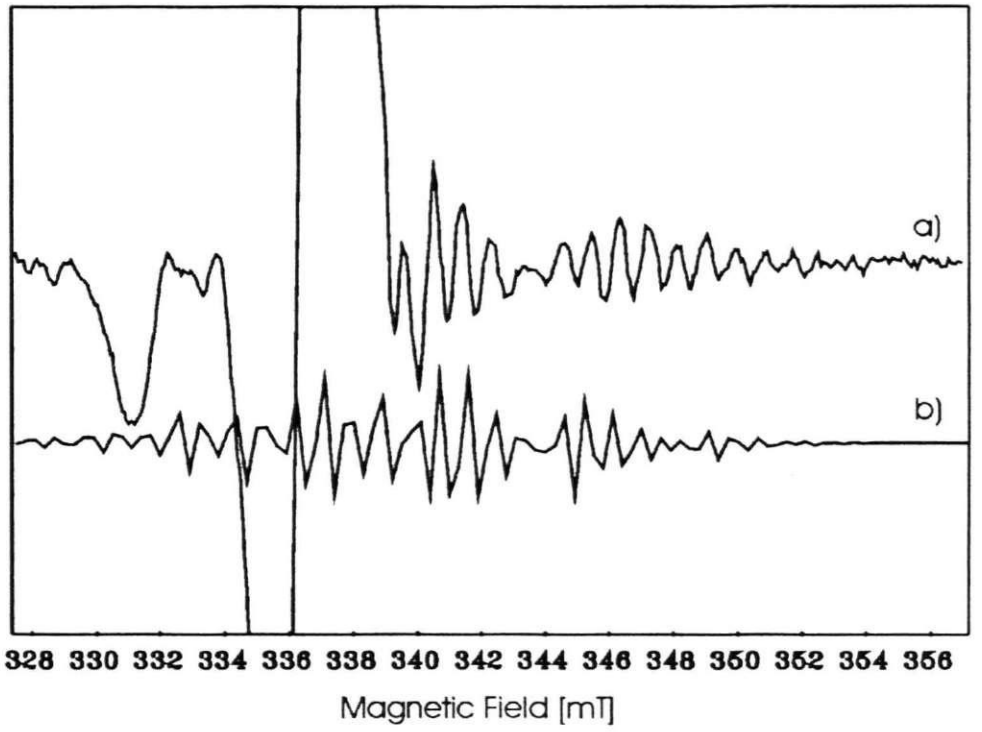


Zīm. 15. F-tipa centra EPR spektri $LiBaF_3$ kristālā <110> virzienā (eksperimentālie- **a** un teorētiskie- **b**).

EPR spektru aprēķinam orientācijā B || [100], izmantojot tabulā 2. dotos spin-Hamiltoniāna parametrus.

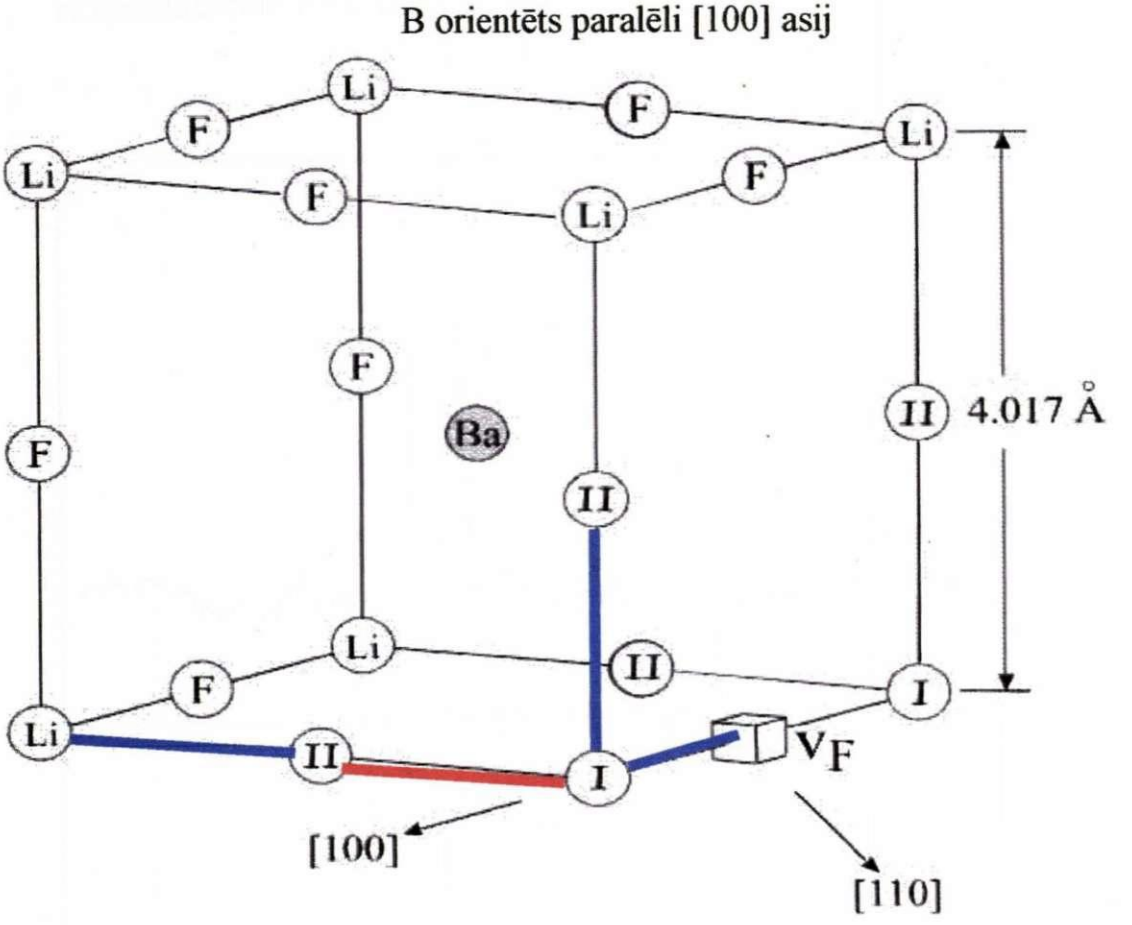


Zīm. 16. F-tipa centra EPR spektra aprēķini <100> virzienā: g-tenzora un hipersīkstruktūras tenzora parametru vērtības dažādām centru orientācijām

| X ($\varphi$=0°) | Y, Z ($\varphi$=90°) |
|---|---|
| $g_{\|\|}$ = 1,990±0,005 | $g_{\perp}$ = 1,960±0,005 |
| 8 F = 95,96 MHz | 4 F = 95,96 MHz |
| 2 Li = 28.87 MHz | 4 F = 75,67 MHz |
| | 2 Li = 22,98 MHz |

17. Zīmējumā aprēķinātie EPR spektri F-tipa centram orientācijāB || [111], salīdzināti ar RT apstarotā $LiBaF_3$ kristāla atbilstošo eksperimentālo EPR spektru.

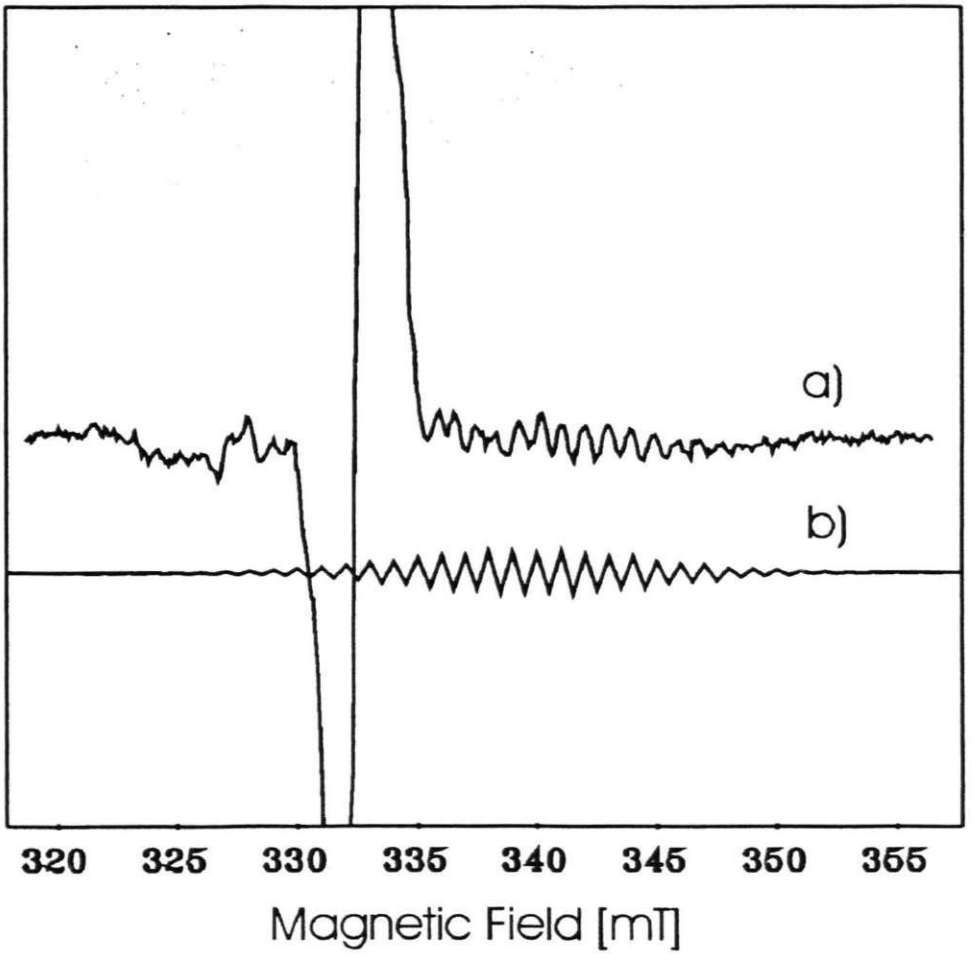


Zīm. 17. F-tipa centra EPR spektri $LiBaF_3$ kristālā <100> virzienā (eksperimentālie- **a** un teorētiskie- **b**)

## 6.4. Secinājumi

Istabas temperatūrā apstarotā $LiBaF_3$ kristāla EPR spektru, kurš sastāv no apmēram 35 līnijām labi izdevies aprakstīt ar F-tipa centra modeli. Nesapārotais spins atrodas fluora vakancē un tā kaimiņu I koordinācijas sfērā atrodas 2 Li kodoli un II koordinācijas sfērā atrodas 8 F kodoli. Ar mūsu darbā piejamajām eksperimentālajām un teorētisko aprēķinu metodēm nav izdevies iegūt informāciju par III un tālākajās koordinācijas sfērās iespējamajām perturbācijām.

7. Aizstāvāmās tēzes

1. 77 K temperatūrā apstarotā $LiBaF_3$ kristālā novērotais EPR spektrs ar g-tenzora asi virzītu [110] virzienā atbilst $V_K$ centram

2. Istabas temperatūrā apstarotā $LiBaF_3$ kristālā novērotais EPR spektrs ar apmēram 35 hipersīkstruktūras līnijām un g-tenzora asi virzītu [100] virzienā atbilst F-tipa centram

## 8. Nobeigums

Promocijas darba mērķis kopumā ir sasniegts un darba uzdevumi izpildīti – darbā ir ar EPR metodi identificēti divi jauni defekti $LiBaF_3$ kristālā. Jāatzīmē, ka darba izpildes gaitā ir novēroti vairāk EPR spektru, nekā tie divi, kurus mums izdevās identificēt. Gan 77 K temperatūrā, gan istabas temperatūrā apstarotajos paraugos neidentificētas palikušas vairākas spēcīgas EPR līnijas magnētisko lauku rajonā ap ~ 330 mT.

Promocijas darba autora ieguldījums veiktajos pētījumos ir: visi darbā izpētīto kristālu asu orientācijas noteikšana ar rentgenstruktūranalīzes metodēm, visu darbā aprakstīto EPR spektru un to leņķisko atkarību mērījumi, kā arī būtisks ieguldījums spektru teorētiskajā modelēšanā, sevišķi F-tipa centru EPR spektru modelēšanā. Tādejādi promocijas darbu var uzskatīt par sekmīgi nobeigtu. Turpmākais darbs dotajā pētījumu virzienā varētu tikt turpināts, mēginot ar EPR un citām metodēm mēginot izpētīt pārejos, mūsu darbā neidentificētos, defektus.

## 9. Literatūras saraksts


1. N.V. Shiran, A.V. Gektin, A.S. Voloshinovski, and V.V. Voronova, Radiation Measurements, 1998, vol. 29, p. 295

2*. I. Tale, H.-J. Fitting, P. Kulis, V. Ogorodnik, U. Rogulis, M. Springis, V. Tale, J. Trokss and A. Veispals, Hole self-trapping and recombination in $LiBaF_3$., Rad. Effects and Defects in Solids, 1999, vol. 149, pp. 269-272

3*. I. Tale, M. Springis, U. Rogulis, V. Ogorodnik, P. Kulis, V. Tale, A. Veispals and H.-J. Fitting, Self-trapped holes in $LiBaF_3$ crystals, Rad. Effects and Defects in Solids, 2001, vol. 155, pp. 51-54

4*. I. Tale, M. Springis, U. Rogulis, V. Ogorodnik, P. Kulis, V. Tale, A. Veispals and H.-J. Fitting, Self-trapped holes and recombination luminescence in $LiBaF_3$ crystals, Radiation Measurements, 2001, vol. 119, pp. 453-458

5*. U. Rogulis, V. Ogorodnik, I.Tale and A.Veispals, EPR of radiation defects in $LiBaF_3$ crystals, Rad. Effects and Defects in Solids, 2002, vol. 157, Nos. 6-12, pp. 699-703

6*. V. Ogorodnik, U. Rogulis, I.Tale and A.Veispals, EPR of F-type centres in $LiBaF_3$, Latvian Journal of Physics and Technical sciences 2004, N 2, pp. 62-67

7. T. Yoshida, H.Aoki, H. Takeuchi, M.Arakawa and K. Horai, J. Phys. Soc. Japan, Letters, 1979, vol. 46, p. 1661

8. M. Yamaga, M. Honda, K.Shimamura, T. Fukuda and T.Yosida, J. Phys.: Condens Matter, 2000, vol. 12, p. 5917

9. Y. Tan, C. Shi, Journal of Physics and Chemistry of Solids, 1999, vol. 60, p. 1805

10. M. Yamaga, T. Imai, K. Shimamura, T. Fakuda, and M. Honda, J. Phys. Condens. Matter, 2000, vol. 12, p. 3431

11. А.В. Геткин, Н.В. Ширан, В.В. Воронова, Тезисы конференции: Твердотельные детекторы ионизирующих излучений, 1997, TTR-97, 37

12. N.V. Shiran, A.V. Gektin, A.S. Voloshinovski, N.N. Voronova, Radiation Measurements, 1998, vol. 29, p. 295

13. A. Wojtowicz, P. Szupryczynski, J. Glodo, J. Phys.: Condens. Matter, 2000, vol. 12, p. 4097

14. Zi-Yuan Yang, J. Phys.: Condens. Matter, 2000, vol. 12, p. 4091

15. N.V. Shiran, A.V. Gektin, O.A. Shepelev, V.V. Voronova, Yu.A. Nesterenko, Radiation Measurements, 2001

16. K. Somaiah, V. Narayana, Matterials Chemistry and Physics, 1990, vol. 24, p. 353

17. A. Meijerink, Journal of Luminescence,1993, vol. 55, p. 125

18. M. Evely., M. Duarte, L.S. Baldochi, P.S. Morato, F. Viera and N.D. Viera Jr., J. Phys. Chem. Solids, 1997, vol. 58, p. 655

19. A.V. Chadwick, S.R. Davis, J.F. Limat, M.E.G. Valerio and S.L. Baldochi, J. Phys: Condens. Matter, 1996, vol. 8, p. 10689

20. A.V. Getkin, N.N. Ivanov, Yu.A. Shiran, V.V. Voronova, Abstr. of the International Conference ICDM'96, Wake Forest 1996, p. 276

21. L. Prado, L. Gomes, S.L. Baldochi, S.P. Morato and N.D. Viera J. Phys. Condens. Matter, 1998, vol. 10, p. 8247

22. P. Kulis, I. Tale, M. Springis, U. Rogulis, J. Trokss, A. Veispals and H.-J. Fitting, Radiation Effects and Deffects in Solids, 1999, vol. 149, p. 99

23. P. Kulis, M. Springis, I. Tale, Annealing of color centers in $LiBaF_3$, Radiation effects and Defects in Solids, 2002, Vol. 157, pp. 737-741

24. V. Ziraps, V. Graveris, P. Kulis, I. Tale, Ion Diffusion-controlled thermally stimulated processes in x-ray irradiated halide crystals, Radiation effects and Defects in Solids, 2002, Vol. 157, pp. 755-759

25. U. Rogulis, J.-M. Spaeth, I. Tale, M. Nikl, N. Ichinose, K. Shimamura, Magnetooptical studies of defects and recombination luminescence in $LiBaF_3$, Radiation Measurements, 2004 (redakcijā)

26. А.С. Марфухин Спектроскопия, Люминесценция и радиационные центры в минералах, Недра, М1975

27. Дж. Вертц, Дж. Болтон, Теория и практические приложения метода ЭПР, Мир, М1975

28. С.А. Альтшулер, Б.М. Козырев, Электронный парамагнитный резонанс соединений элементов промежуточных групп, Наука, М1972

29. R. Kaplan, P.J. Bray, Phys. Rev., 1963, vol. 129, pp. 1919-2935.

The luminescence bands at 300–370 nm may be caused by charge-transfer transitions between F-type and $V_K$ centres.

## *References*

[1] A.V. Gektin, N.N. Ivanov, Yu.A. Nesterenko, N.V. Shiran and V.V Voronova, Abstracts of the Int. Conf. ICDIM'96, Wake Forest, 1996, p. 276.
[2] N.V. Shiran, A.V. Gektin, V.K. Komar and V.V. Voronova, Abstracts of the Int. Conf. ICL'96, Prague, 1996, p. 8–195.
[3] L. Prado, L. Gomes, S.L. Baldochi, S.P. Morato and N.D. Vieira, Jr., *J. Phys.: Condens. Matter* **10**, 8247 (1998).
[4] K. Somaiah, M. Venkata Narayana and L.H. Brixner, *Materials Chemistry and Physics* **24**, 353 (1990).
[5] Th. Pawlik, Doctoral Thesis, Paderborn (1996).
[6] J.J. Rosseau and J.C. Fayet, *Phys. Stat. Sol. (b)* **77**, 195 (1976).
[7] L.E. Halliburton and E. Sonder, *Solid State Communications* **21**, 445 (1969).
[8] T.P.P. Hall, *Brit. J. Appl. Phys.* **17**, 1011 (1966).
[9] E. Kotomin, I. Tale, V. Tale, P. Butlers and P.Kulis, *J. Phys.: Condens. Matter* **1**, 6777 (1989).

# HOLE SELF-TRAPPING AND RECOMBINATION IN $LiBaF_3$

I. TĀLE[a], H.-J. FITTING[b], P. KŪLIS[a], V. OGORODNIK[a], U. ROGULIS[a,*], M. SPRIŅĢIS[a], V. TALE[a], J. TROKŠS[a] and A. VEISPĀLS[a]

[a]*Institute of Solid State Physics, University of Latvia, Kengaraga Str. 8, LV-1063 Riga, Latvia;* [b]*Fachbereich Physik, Universität Rostock, D-18051 Rostock, Germany*

*(Received 6 July 1998; In final form 20 September 1998)*

We investigated the electron paramagnetic resonance (EPR), recombination afterglow and thermostimulated luminescence (TSL) of the X-irradiated $LiBaF_3$ crystals. After X-irradiation at 80 K, an EPR of the self-trapped hole centre $V_K(F_2)$ oriented along the [110] axis is identified. X-irradiation at temperatures below 200 K results in a creation of a long-term temperature-independent afterglow – tunnelling luminescence (TL), with main emission bands at 300, 370 and 430 nm. The short wavelength TL bands are associated with the tunnelling recombination of the electron centre with the $V_K$ centre, with thermal stability estimated to be about 130 K.

*Keywords:* $LiBaF_3$; Self-trapped holes; Recombination luminescence; EPR

$LiBaF_3$ crystal is expected to find application as a material for thermal neutron detection [1] and X-ray storage phosphors [2]. However, there is little information [3] about the defect centres and recombination processes in these crystals. Somaiah *et al.* [4] suggested that even at room temperature $V_K$ centres contribute to the X-ray excited luminescence. The aim of the present work was to study the origin and the recombination processes of the hole centres created by the ionising irradiation.

* Corresponding author.

After X-irradiation of single $LiBaF_3$ crystal at 80 K, the EPR spectrum shows spectral patterns corresponding to axial centres oriented along the [110] axis (Fig. 1). Splittings in the spectrum can be explained by a hyperfine (hf) interaction of the unpaired spin $S = 1/2$ with two fluorine nuclei ($I = 1/2$ with a natural abundance 100%).

The first estimations of the $F^{19}$ hf interaction parameters from the EPR angular dependencies ($A_\parallel = 2550$ MHz, $A_\perp = 300$ MHz) are in good agreement with the parameters for $V_K$ (fluorine $F_2^-$) centres found in other perovskite crystals [5–8]. No EPR signal of $V_K$ centres was observed after X-irradiation at room temperature, therefore such centres are not stable in $LiBaF_3$ at room temperature.

X-irradiation below 200 K results in the creation of a long-term temperature-independent afterglow, as observed, by subsequent cooling down to 80 K and corresponding to the radiative charge-transfer-recombination between close electron and hole centres (i.e. tunnelling luminescence (TL)). The TL spectrum is characterised by 300, 370 and 430 nm bands (Fig. 2). The 300, 370 nm TL bands diminish both by the

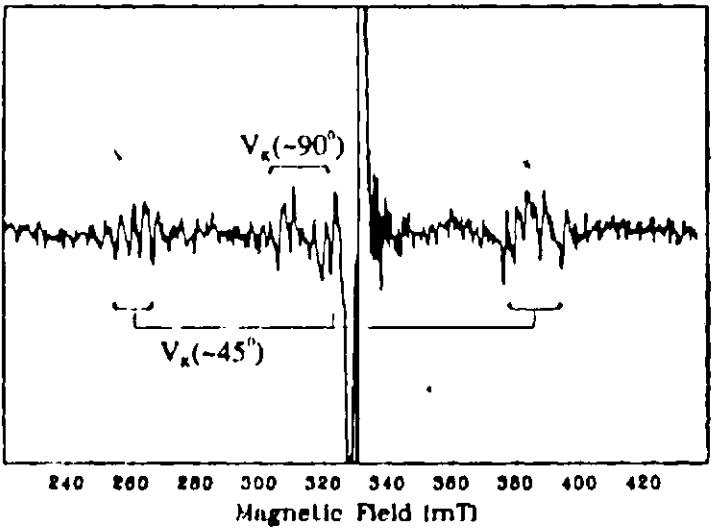


FIGURE 1 The EPR spectrum at 80 K of the $LiBaF_3$ crystal after X-irradiation at 80 K. Microwave frequency 9.18 GHz. The orientation of the crystal is approximately 5° deviated from the $B_0$ [100]. ~45° and ~90° oriented $V_K$ centres are shown, the lines are split due to the crystal disorientation. Central strong lines belong to unidentified radiation defects.

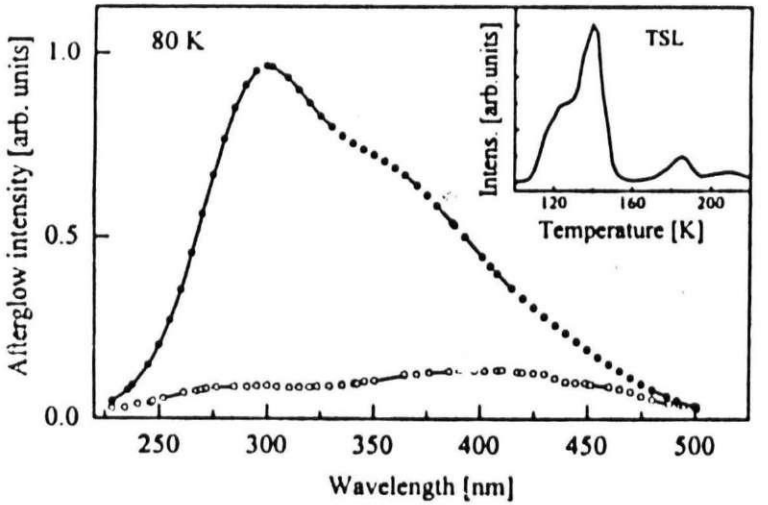


FIGURE 2 The afterglow spectra at 80 K of the $LiBaF_3$ crystal after X-irradiation at 80 K (solid circles) and 160 K (open circles). Inset: the TSL curve of the $LiBaF_3$ crystal after X-irradiation at 80 K.

rise of X-irradiation temperature as well as by the heating of the sample preliminary X-irradiated (at 80 K) above the 130 K TSL peak (Fig. 2, inset).

In the early stages of the 130–140 K TSL peak, the diffusion-controlled-tunnelling-recombination kinetics occurs, as discussed in the case of halide crystals in [9]. A small step-like (2–5 K) increase of the stimulation temperature leads to the long-term increase of the recombination luminescence to the quasi-stationary value. The transition time to the new quasi-stationary recombination decreases with increased stimulation temperature. Thus, the process involves the diffusion of the reaction partners leading to radiative charge transfer between close pairs with a probability exponentially increasing with decreasing pair separation.

Based on the obtained data the following conclusions can be drawn:

In $LiBaF_3$ crystals self-trapping of holes occurs in the form of fluorine $F_2^-$ molecular $V_K$ centres occupying the fluorine site and oriented along [110] direction.

The thermoactivated migration of the $V_K$ centre occurs starting from $\sim$ 100 K via reorientation hops, without breaking the molecular bond. Above 130 K the $V_K$ centres are thermally destroyed.

# SELF-TRAPPED HOLES IN $LiBaF_3$ CRYSTALS

I. TALE[a]*, M. SPRINGIS[a], U. ROGULIS[a], V. OGORODNIK[a], P. KULIS[a], V. TALE[a], A. VEISPALS[a] and H.-J. FITTING[b]

[a]*Institute of Solid State Physics, University of Latvia, LV-1063, Riga, Latvia;*
[b]*Physics Department, University of Rostock, Universitätsplatz 3, Rostock, German*

*(Received 7 April 2000)*

Self-trapped holes ($V_K$-centres) in x-irradiated $LiBaF_3$ crystals were investigated by electron paramagnetic resonance (EPR), recombination afterglow and thermostimulated luminescence (TSL). After x-irradiation at 77 K, an EPR of the self-trapped hole centre $V_K$ ($F_2^-$) oriented along the [110] axis is identified. The $^{19}F$ hyperfine interaction parameters of $V_K$-centres estimated from EPR angular dependencies are: $A_{\parallel} = 2520$ MHz; $A_{\perp} = 200$ MHz; the g-tensor parameters are: $g_{\parallel} = 2.002$ and $g_{\perp} = 2.024$. X-irradiation at temperatures below 200 K results in a creation of a long-term temperature-independent afterglow-tunnelling luminescence (TL), with main emission bands at ~4.1 eV and ~3.15 eV. The short wavelength TL bands are associated with the tunnelling recombination of the electron centre with the $V_K$-centre, with thermal stability estimated to be about 130 K.

*Keywords:* $LiBaF_3$; EPR; Self-trapped holes; Recombination luminescence

$LiBaF_3$ crystal is expected to find application as a material for thermal neutron detection and storage phosphors (*e.g.* [1]). Intrinsic electron trap centres, F- and F- aggregate centres in $LiBaF_3$ crystals, have already been studied in detail [2, 3]. Recently we observed the EPR of the self-trapped holes, $V_K$-centres in $LiBaF_3$ crystals, after x-irradiation at liquid nitrogen temperature [4]. In this article we present a detailed EPR investigation of the $V_K$-centres in $LiBaF_3$ crystal and discuss their recombination processes.

*Corresponding author. E-mail: itale@latnet.lv

$LiBaF_3$ crystals were grown using monocrystalline LiF and $BaF_2$ as a raw material. X-ray structure analysis showed that $LiBaF_3$ crystals tend to grow in a mosaic-type polycrystalline blocks. For EPR measurements, single crystalline blocks were separated.

Figure 1 shows the experimental angular dependence of the EPR lines (open squares) of $LiBaF_3$ single crystal after x-irradiation at 77 K. The crystal was rotated in a plane, which makes an angle of 23° with the (001) plane of the crystal. No experimental line positions are shown at magnetic fields around 330 mT because of the overlapping with unidentified strong EPR lines. At each angle we observe six pairs of EPR lines positioned

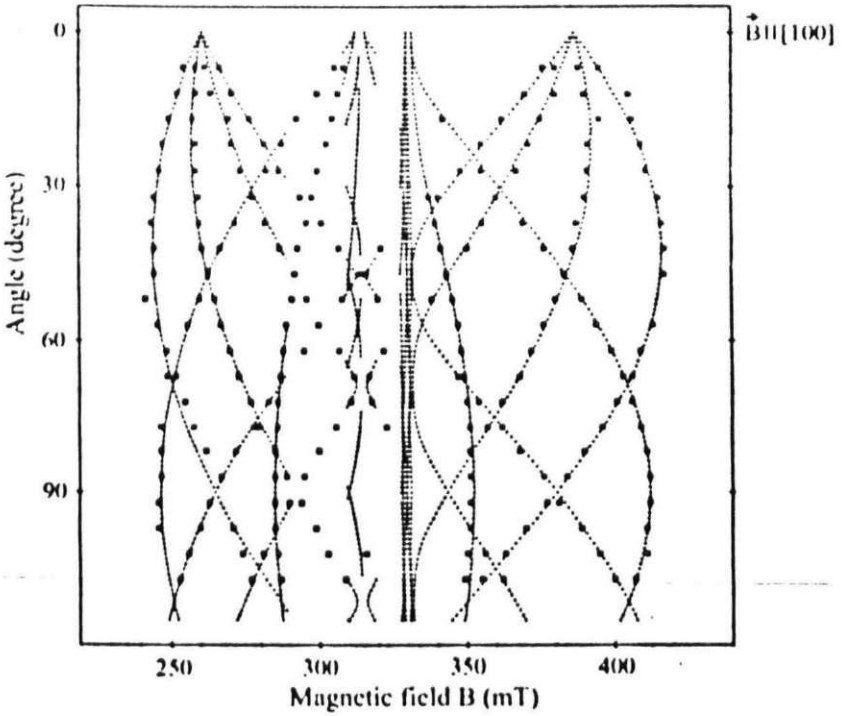


FIGURE 1 EPR angular dependence of the $LiBaF_3$ crystal after x-irradiation at 77 K. Crystal was rotated in the plane, which makes an angle of 23° with the (001) plane of the crystal. At 0 B is parallel to [100] axis and at 90 B makes an angle of 23° with the [010] axis of the crystal. The open squares represent the experimental line position; the dashed lines are calculated by using the parameters of Table I. No experimental line positions are shown at magnetic fields around 330 mT because of the overlapping with strong unidentified EPR lines. The spectra were recorded at 77 K applying a microwave frequency of 9.18 GHz.

nearly symmetrically to the magnetic field value 330 mT. Four of six lines in each pair are going together for a rotation towards B parallel to [100] axis. This indicates that we deal here with only one centre with six different centre orientations; four of them are magnetically equivalent to B parallel to [100]. This behaviour corresponds to axial centres oriented along the [110] axis; splittings in the spectrum can be explained by a hyperfine (*hf*) interaction of the unpaired spin $S = 1/2$ with two fluorine $^{19}F$ nuclei ($I = 1/2$ with a natural abundance 100%). In Figure 1 the dashed lines are calculated EPR line positions by using the conventional spin-Hamiltonian of the $V_K$ (fluorine $F_2^-$) centre. The estimated $^{19}F$ *hf* interaction parameters of $V_K$-centres in $LiBaF_3$ crystals are: $A_{\parallel} = 2520$ MHz; $A_{\perp} = 200$ MHz; the *g*-tensor parameters are $g_{\parallel} = 2.002$ and $g_{\perp} = 2.024$. The parameters are collected in Table I, together with the parameters for $V_K$-centres reported on similar perovskite crystals [5–7].

The spin-Hamiltonian parameters of $V_K$-centres in $LiBaF_3$ crystals are in good agreement with the other perovskite crystals. Special attention could be paid to the *g*-shift: $\Delta g = g_{\perp} - g_{\parallel}$, which in the case of $V_K$-centres has a value of about $\Delta g = 0.02$. For H-centres ($F_2^-$ occupying one fluorine site) in perovskites [7–9] the $\Delta g$ is nearly halved and has a value of about $\Delta g = 0.01$; also the *hf* interaction parameter $A_{\parallel}$ for H-centre is usually larger than that of the $V_K$-centres. Our estimated value of $\Delta g = 0.022 \pm 0.004$ agrees well with the $\Delta g$ values for $V_K$-centres in perovskites, but not for H-centres; therefore in $LiBaF_3$ crystals we indeed observed the $V_K$-centres.

$V_K$-centres participate in low temperature recombination processes. After x-irradiation at temperatures below 200 K, a long-term temperature-independent afterglow-tunnelling luminescence (TL) occurs, with main emission bands at ~4.1 eV and ~3.15 eV. The ~4.1 eV TL band diminish both by the rise of x-irradiation temperature as well as by the

TABLE I Parameters of the spin Hamiltonian of $V_K$-centres in $LiBaF_3$ and similar perovskite crystals

| *Crystal* | $A_{\parallel}$ (MHz) | $A_{\perp}$ (MHz) | $g_{\parallel}$ | $g_{\perp}$ | *Reference* |
|---|---|---|---|---|---|
| $LiBaF_3$ | $2520 \pm 20$ | $200 \pm 30$ | $2.002 \pm 0.002$ | $2.024 \pm 0.002$ | present work |
| $KMgF_3$ | $2474 \pm 6$ | $159 \pm 6$ | 2.0024 | 2.021 | [5] |
| $RbCaF_3$ | $2563 \pm 9$ | $28 \pm 28$ | 2.003 | 2.023 | [6] |
| $CsCaF_3$ | $2509 \pm 2$ | $51 \pm 10$ | 2.0031 | 2.0244 | [7] |

heating of the sample, preliminary x-irradiated (at 77 K), above the 130 K thermostimulated luminescence (TSL) peak. We consider that the TL band at ~4.1 eV is associated with the tunnelling recombination of the electron centre, probably F-type centre, with the $V_K$-centre, with thermal stability estimated to be about 130 K. In the early stages of the 130–140 K TSL peak, the characteristic diffusion-controlled-tunnelling-recombination kinetics occur, as discussed in the case of halide crystals in [10]. A small step-like (2–5 K) increase of the stimulation temperature leads to the long-term-increase of the recombination luminescence to the quasi-stationary value. The transition time to the new quasi-stationary recombination decreases with increased stimulation temperature. Thus, the process involves the diffusion of the reaction partners leading to radiative charge-transfer between close pairs with a probability exponentially increasing with decreasing pair separation. We propose that the thermoactivated migration of the $V_K$-centre occurs starting from ~100 K via reorientation hops, without breaking the molecular bond; above 130 K the $V_K$-centres are thermally destroyed.

## *References*


[1] Shunin, N. V., Gektin, A. V., Voloshinovski, A. S. and Voronova, V. V. (1998) *Radiation Measurements*, **29**, 295.

[2] Tale, I., Kulis, P., Rogulis, U., Tale, V., Trokss, J., Veispals, A., Barboza-Flores, M. and Luthy, H.-J. (1997) *J. Luminescence*, **72–74**, 722.

[3] Prado, L., Gomes, L., Hakkuchi, S. L., Morato, S. P. and Vieira Jr, N. D., (1998) *J. Phys.: Condens. Matter*, **10**, 8247.

[4] Tale, I., Luthy, H.-J., Kulis, P., Ogorodnik, V., Rogulis, U., Springis, M., Tale, V., Trokss, J. and Veispals, A., (1999) *J. Luminescence*, **149**, 269.

[5] Hall, T. P. P. (1966) *Brit. J. Appl. Phys.*, **17**, 1011.

[6] Halliburton, L. E. and Sonder, E., (1977) *Solid State Communications*, **21**, 445.

[7] Pawlik, Th., (1996) *Doctoral Thesis, Paderborn*.

[8] Rose, B. H., Rhoads, J. E. and Halliburton, L. E., (1976) *Phys. Rev. B*, **14**, 3583.

[9] Halliburton, L. E., Jafari, A. and Burris, R. A., (1981) *Phys. Rev. B*, **23**, 6765.

[10] Kotomin, E., Tale, I., Tale, V., Butlers, P. and Kulis, P., (1989) *J. Phys.: Condens. Matter*, **1**, 6777.

*Radiation Effects & Defects in Solids*, Vol. 153, pp. 53–59
Reprints available directly from the publisher
Photocopying permitted by license only



# CRYSTAL-SIZE DEPENDENCE OF LUMINESCENCE AND ABSORPTION SPECTRA OF F($Br^-$) AND F($F^-$) CENTERS IN BraFBr

Y. KONDO[a,*], T. TEZUKA[a] and Y. IWABUCHI[b]

[a]*Department of Applied Physics, Tohoku University, Aobaku, Sendai, Miyagi 980-8579, Japan;* [b]*Miyanodai Technology Development Center, Fuji Photo Film Co., Ltd., Miyanodai, Kaisei, Kanagawa 258*

*(Received 7 April 2000)*

Luminescence and absorption spectra of F($Br^-$) and F($F^-$) centers have been measured in various sizes of BaFBr crystals. Formation efficiency and the luminescence intensity of F($F^-$) were almost the same in all sizes of the crystals, while the intensity of the F($Br^-$) luminescence decreased with decreasing size. In the finest powdered crystal (used in image plates IP), the F($Br^-$) luminescence was not detected. Since the F($Br^-$) center is considered to be mobile at room temperature, RT, the nonexistence of the F($Br^-$) luminescence and the production of stable F($Br^-$) centers in the IP can be attributed to the pinning of the F($Br^-$) centers at the surface of the crystal.

*Keywords:* X-ray imaging; Storage phosphors; Color center; Ionic crystals; BaFBr

Since the first commercial application of BaFBr:Eu to recording two-dimensional X-ray images was reported by the Fuji Photo Film Co., Ltd. [1], almost two decades have passed. Although many studies have been done to look for better materials, so far BaFBr:Eu is still the best storage phosphor for X-rays. However, the image plate, IP, has a few drawbacks such as fading of the recorded images, afterglow, and the reappearance of the erased images. Among these, fading may be the most serious draw-

*Corresponding author. E-mail: kondo@laser.apph.tohoku.ac.jp

PERGAMON

Radiation Measurements 33 (2001) 751–754

Radiation Measurements

www.elsevier.com/locate/radmeas

# Self-trapped holes and recombination luminescence in $LiBaF_3$ crystals

I. Tale[a], M. Springis[a], U. Rogulis[a,*], V. Ogorodnik[a], P. Kulis[a], V. Tale[a], A. Veispals[a], H.-J. Fitting[b]

[a] *Institute of Solid State Physics, University of Latvia, 8 Kengaraga Str., LV-1063, Riga, Latvia*
[b] *Physics Department, University of Rostock, Universitätsplatz 3, Rostock, Germany*

Received 20 August 2000; received in revised form 5 February 2001; accepted 16 February 2001

**Abstract**

We investigated electron paramagnetic resonance (EPR) angular dependencies, recombination afterglow and thermostimulated luminescence of undoped $LiBaF_3$ crystals, X-irradiated at low temperatures. EPR parameters of the $F_2^-$ molecule oriented along the [1 1 0] direction have been obtained. Based on the value of the $g$-shift $\Delta g = g_\perp - g_{II} = 0.02$, characteristic for the $V_K$-centres in similar perovskites, we propose that we indeed observed the $V_K$-centres, not the H-centres. X-irradiation below 170 K results in creation of a long-time temperature-independent afterglow due to the tunnelling recombination between close electron and hole centres. The F-type electron centres and the $V_K$ as well as probably $O^{2-}$ centres are proposed to be the tunnelling recombination partners, responsible for the 4.1 and 3.15 eV luminescence bands, respectively.

*Keywords:* $LiBaF_3$; EPR; Self-trapped holes; Recombination luminescence

## 1. Introduction

$LiBaF_3$ represents a group of materials, prospective as scintillators and as radiation memory materials for dosemetric purpose. Well-known cross luminescence bands in ultraviolet have been found in $LiBaF_3$ crystals by X-ray and electron beam irradiation (Knitel et al., 1996; Melchakov et al., 1990; Rodnyi et al., 1991). In undoped crystals we have recently observed several additional luminescence bands of unknown origin. The broad luminescence band between 250 and 400 nm is proposed to be due to the self-trapped excitons (Tale et al., 1997). It can be expected, that intrinsic defects can cause other radiative electron transitions. Intrinsic electron trap centres, F- and F- aggregate centres in $LiBaF_3$ crystals, have already been studied in detail (Tale et al., 1997; Prado et al., 1998). F-type colour centres are the main radiation defects created by X-irradiation at room temperature (Tale et al., 1997; Kulis et al., 1999). Recently electron paramagnetic resonance (EPR) of $V_K$-centres in undoped crystals has been reported after X-irradiation at liquid nitrogen temperature (Tale et al., 1999). In this article we present detailed EPR investigations of the $V_K$-centres in $LiBaF_3$ crystal and discuss the origin of the recombination luminescence.

## 2. Experimental

$LiBaF_3$ crystals were grown using monocrystalline LiF and $BaF_2$ as a raw material. X-ray structure analysis showed that $LiBaF_3$ crystals tend to grow in mosaic-type polycrystalline blocks. For EPR measurements, single crystalline blocks were separated.

The samples were X-irradiated using a W-anode X-ray tube operated at 45 kV, 10 mA. The thermostimulated

* Corresponding author. Fax: +371-711-2583.
*E-mail address:* rogulis@latnet.lv (U. Rogulis).

1350-4487/01/$ - see front matter 
PII: S1350-4487(01)00096-8

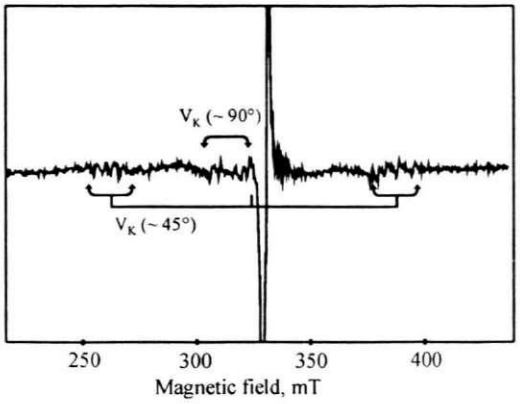


Fig. 1. The EPR spectrum at 77 K of the $LiBaF_3$ crystal after X-irradiation at 77 K. Microwave frequency 9.18 GHz. The orientation of the crystal is approximately 5° deviated from the B || [1 0 0]. ~ 45° and ~ 90° oriented $V_K$-centres are shown. The lines are split due to the crystal disorientation. Central strong lines belong to unidentified radiation defects.

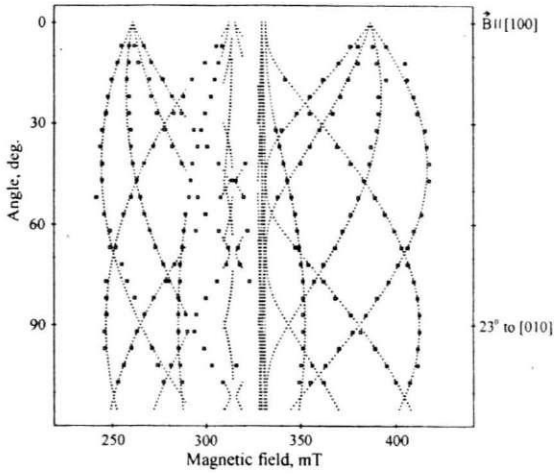


Fig. 2. EPR angular dependence of the $LiBaF_3$ crystal after X-irradiation at 77 K. The crystal was rotated in the plane, which makes an angle of 23° with the (0 0 1) plane of the crystal. At 0° B is parallel to [1 0 0] axis and at 90° B makes an angle of 23° with the [0 1 0] axis of the crystal. The open squares represent the experimental line position; the dashed lines are calculated by using the parameters of Table 1.

luminescence (TL) was recorded at heating rate 0.1 K/s. EPR measurements were performed using an RE-1306 spectrometer.

## 3. Results

The EPR spectrum of the $LiBaF_3$ single crystals X-irradiated at 77 K shows spectral patterns corresponding to axial centres oriented along the [1 1 0] axis (Fig. 1). Splitting in the spectrum can be explained by a hyperfine (hf) interaction of the unpaired spin $S = \frac{1}{2}$ with two fluorine nuclei ($I = \frac{1}{2}$ with a natural abundance 100%).

Fig. 2 shows the experimental angular dependence of the EPR lines (open squares) of a $LiBaF_3$ crystal after X-irradiation at 77 K. The crystal was rotated in the plane, which makes an angle of 23° with the (0 0 1) plane of the crystal. No experimental line positions are shown at magnetic fields around 330 mT because of the overlapping with unidentified strong EPR lines. At each angle we observe six pairs of EPR lines positioned nearly symmetrically to the magnetic field value of 330 mT. Four of six lines in each pair are going together for a rotation towards B parallel to [1 0 0] axis. This indicates that we deal here with only one centre with six different centre orientations; four of them are magnetically equivalent for B parallel to [1 0 0]. This behaviour corresponds to axial centres oriented along the [1 1 0] axis. In Fig. 2 the dashed lines are calculated EPR line positions by using of the conventional spin-Hamiltonian of the $V_K$ (fluorine $F_2^-$) centre. The estimated $^{19}F$ hf interaction parameters of $V_K$-centres in $LiBaF_3$ crystals are: $A_{II} = 2520$ MHz; $A_\perp = 200$ MHz; the $g$-tensor parameters are $g_{II} = 2.002$ and $g_\perp = 2.024$. The parameters are collected in Table 1, together with the parameters for $V_K$-centres reported on similar perovskite crystals.

X-irradiation below 170 K results in creation of a long-term temperature-independent afterglow, i.e. the tunnelling luminescence (TuL) appears (Kotomin et al., 1989). The TuL spectrum sufficiently depends on the X-irradiation temperature. In the whole temperature interval the

Table 1
Parameters of the spin Hamiltonian of $V_K$-centres in $LiBaF_3$ and similar perovskite crystals

| Crystal | $A_{\|}$ (MHz) | $A_\perp$ (MHz) | $g_{\|}$ | $g_\perp$ | Reference |
|---|---|---|---|---|---|
| $LiBaF_3$ | 2520 ± 20 | 200 ± 30 | 2.002 ± 0.002 | 2.024 ± 0.002 | Present work |
| $KMgF_3$ | 2474 ± 6 | 159 ± 6 | 2.0024 | 2.021 | Hall (1966) |
| $RbCaF_3$ | 2563 ± 9 | 28 ± 28 | 2.003 | 2.023 | Halliburton and Sonder (1977) |
| $CsCaF_3$ | 2509 ± 2 | 51 ± 10 | 2.0031 | 2.0244 | Pawlik (1996) |

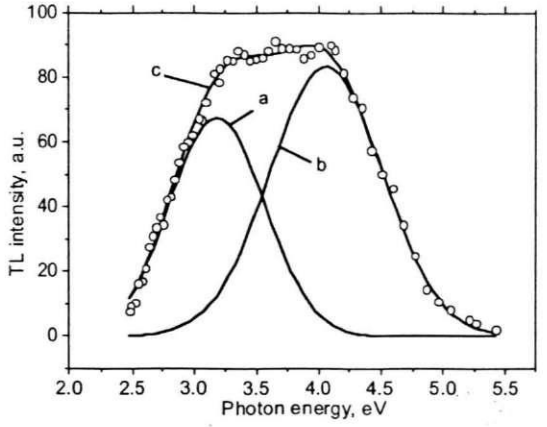


Fig. 3. Curve fit by Gaussians of the TuL spectrum observed at 80 K after cooling down from the excitation temperature at 100 K: (a) TuL band at $h\nu = 4.1$ eV, (b) TuL band at $h\nu = 3.15$ eV, (c) sum fitted spectra, open circles: experimental TuL spectrum.

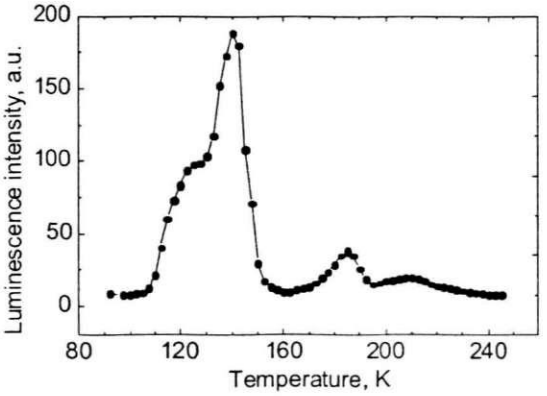


Fig. 4. TL of $LiBaF_3$ crystal X-irradiated at 80 K.

composite band represents the TuL indicating that several radiative transitions are involved in the TuL. In Fig. 3 two typical TuL spectra obtained after X-irradiation at 100 K are presented. The best fit of the TuL spectrum created at 100 K was achieved assuming presence of two elementary TuL bands at approximately 3.15 eV (curve a) and 4.1 eV (curve b). Increase of the X-irradiation temperature results both in the decrease of the TuL intensity and the change of shape of the TuL spectra. A similar continuous diminishing of the TuL intensity occurs by heating of the sample, X-irradiated at 80 K, to various temperatures followed by cooling down to LNT. The TuL completely vanishes above 170 K. It corresponds to the complete emptying of traps responsible for the 140 K TL peak (Fig. 4). We investigated TL of various undoped $LiBaF_3$ crystals X-irradiated at 80 K. In the temperature region below RT the TL curve in the samples containing F-type centres is represented by four peaks at about 125, 140, 185 and 210 K.

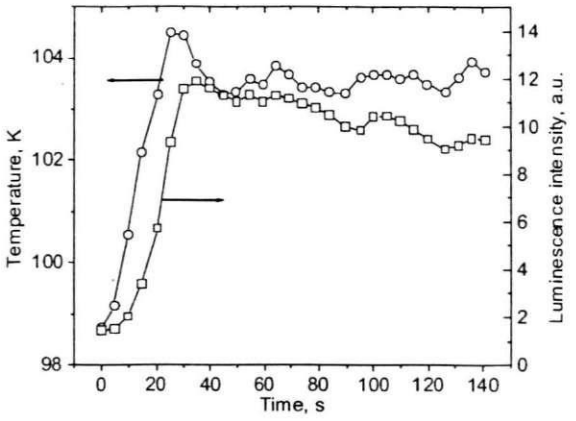


Fig. 5. The simultaneous records of the temperature ($T$) and TL intensity ($I$) by step-like heating of the $LiBaF_3$ sample X-irradiated at 80 K in the early stages of the 120 K TL peak.

In the early stages of the 130–140 K TL peak diffusion-controlled tunnelling-recombination occurs. A small step-like (2–5 K) increase of the stimulation temperature leads to the long-term increase of the recombination luminescence to the quasi-stationary value. Fig. 5 represents the simultaneous records of the time dependence of both the temperature and the TL intensity increase. At the early stage of the 120 K peak (Fig. 5) the increase of the TL intensity is delayed with respect to the increase of temperature. The transition time to the new quasi-stationary recombination decreases with increased stimulation temperature. The conclusion can be drawn that the recombination process responsible for the 120 K TL peak involves the random walk of one of the reaction partners. Decrease of the reaction partner separation leads to radiative charge-transfer between close pairs with a probability exponentially increasing with decreasing pair separation (Kotomin et al., 1989). For the given diffusion rate the recombination rate and the corresponding pair separation distribution function can be characterised by the corresponding mean recombination radius, which decreases by increase of the diffusion rate constant, i.e. temperature. Step-like increase of temperature causes redistribution of the pair separation function. Thus, the new mean recombination radius and corresponding quasi-stationary recombination rate will be reached with some time delay.

## 4. Discussion

The spin-Hamiltonian parameters of $V_K$-centres in $LiBaF_3$ crystals are in good agreement with the other perovskite crystals. Special attention could be paid to the $g$-shift: $\Delta g = g_\perp - g_{II}$, which in the case of $V_K$-centres has a value of about $\Delta g = 0.02$. For H centres ($F_2^-$ occupying one fluorine site) in perovskites (Pawlik, 1996; Rose et al.,

1976; Halliburton et al., 1981) the $\Delta g$ is nearly halved and has its value of about $\Delta g = 0.01$; also the hf interaction parameter $A_{II}$ for H-centres is usually larger than that of the $V_K$-centres. Our estimated value of $\Delta g = 0.022 \pm 0.004$ agrees well with the $\Delta g$ values for $V_K$-centres in perovskites, but not for H centres; therefore in $LiBaF_3$ crystals we indeed observed the $V_K$-centres.

$V_K$-centres participate in low temperature recombination processes. After X-irradiation at temperatures below 200 K, TuL consists of two main emission bands at $\sim$ 4.1 and $\sim$ 3.15 eV. The 4.1 eV TuL band diminishes both by raising the X-irradiation temperature and by heating of the sample, preliminarily X-irradiated (at 77 K), above the 130 K TL peak. We consider that the TuL band at $\sim$ 4.1 eV is associated with the tunnelling recombination of the electron centre, probably F-type centre, with the $V_K$-centre, with a thermal stability estimated to be about 130 K.

The diffusion-controlled-tunnelling-recombination kinetics in $LiBaF_3$ crystals indicates that the thermoactivated migration of the $V_K$-centres occurs starting from $\sim$ 100 K via reorientation hops, without breaking the molecular bond. Either the 60° or the 90° hops can occur in $LiBaF_3$ lattice. Above 130 K the $V_K$-centres are thermally destroyed. The F-type centres are the main electron centres simultaneously created by ionising radiation with the $V_K$-centres. It is reasonable to propose that the 120 K TL peak is due to the radiative diffusion-controlled-tunnelling-recombination of $V_K$-centre and F-type centre pairs. Spontaneous electron transfer from F-type to $V_K$-centre results in the photon emission. The radiative transitions can be either direct ones between the ground states of the electron and hole centres or two step processes via excited state of $V_K$-centres. In the latter case the luminescence of self-trapped excitons will occur. Energy of the TuL band coincides with the self-trapped exciton emission energy reported in (Tale et al., 1997).

We propose that the TuL band at 3.15 eV originates from electron-tunnelling transfer between F-type centers and trace impurity centres. The spectral position of these centres is close to the blue luminescence band discussed in (Springis et al., 1999). The spectral position of the blue luminescence band and its excitation is similar to those, caused by oxygen in other fluorides (Jacobs and Song, 1980). $O^{2-}$ incorporated in an $F^-$ site without charge compensation will act as acceptor.

## References


Hall, T.P.P., 1966. The structure of the self-trapped hole in $KMgF_3$. Br. J. Appl. Phys. 17, 1011–1018.

Halliburton, L.E., Jafari, A., Burris, R.A., 1981. Structure of the H and $H_A$ centers in $RbCaF_3$. Phys. Rev. B 23, 6765–6772.

Halliburton, L.E., Sonder, E., 1977. $V_K$-centres in $RbCaF_3$: lattice distortion in the tetragonal phase. Solid State Commun. 21, 445–447.

Jacobs, P.W.M., Song, K.S., 1980. Thermal depolarisation in crystals of calcium fluoride doped with oxygen. J. Phys. Chem. Solids 41, 437–441.

Knitel, M.J., Dorenbos, P., de Haas, J.T.M., van Eijk, C.W.E., 1996. $LiBaF_3$, a thermal neutron scintillator with optimal n-gamma discrimination. Nucl. Instr. and Meth. A 374, 197–201.

Kotomin, E., Tale, I., Tale, V., Butlers, P., Kulis, P., 1989. Kinetics of non-steady state diffusion-controlled tunnelling recombination of defects in insulating crystals. J. Phys.: Condens. Matter 1, 6777–6785.

Kulis, P., Tale, I., Springis, M., Rogulis, U., Trokss, J., Veispals, A., Fitting, H.-J., 1999. F-type centres in $LiBaF_3$ crystals. Radiat. Eff. Def. Solids 149, 97–100.

Melchakov, E.N., Petrova, M.A., Podkolzina, I.G., Rodnyi, P.A., Terekhin, M.A., 1990. Intrinsic luminescence of $BaLiF_3$ and $BaMgF_4$ crystals. Opt. Spectrosc. 69, 807–808.

Pawlik, Th., 1996. Magnetische Resonanzuntersuchungen an Röntgenspeicherleuchtstoffen mit Perowskit- und Elpasolit-Struktur. Doctoral Thesis, Paderborn, pp. 1–193.

Prado, L., Gomes, L., Baldochi, S.L., Morato, S.P., Vieira Jr, N.D., 1998. Electron-irradiation-induced defects in $LiBaF_3$ crystals. J. Phys.: Condens. Matter 10, 8247–8256.

Rodnyi, P.A., Terekhin, M.A., Melchakov, E.N., 1991. Radiative core-valence transitions in barium based fluorides. J. Lumin. 47, 281–284.

Rose, B.H., Rhoads, J.E., Halliburton, L.E., 1976. Structure of the H center in $KMgF_3$. Phys. Rev. B 14, 3583–3588.

Springis, M., Kulis, P., Tale, I., Veispals, A., Fitting, H.J., 1999. Defect luminescence of $LiBaF_3$ perovskites. In: Mikhailin, V. (Ed.), Proceedings of the 5th International Conference on Inorganic Scintillators and their Application. Moscow State University, Russia, pp. 555–559.

Tale, I., Fitting, H.-J., Kulis, P., Ogorodnik, V., Rogulis, U., Springis, M., Tale, V., Trokss, J., Veispals, A., 1999. Hole self-trapping and recombination in $LiBaF_3$. Radiat. Eff. Def. Solids 149, 269–272.

Tale, I., Kulis, P., Rogulis, U., Tale, V., Trokss, J., Veispals, A., Barboza-Flores, M., Fitting, H.J., 1997. Colour centres in $LiBaF_3$. J. Lumin. 72–74, 722–723.

*Radiation Effects & Defects in Solids*, 2002, Vol. 157, pp. 699–703



# EPR OF RADIATION DEFECTS IN $LiBaF_3$ CRYSTALS

U. ROGULIS*, V. OGORODNIK, I. TALE and A. VEISPALS

*Institute of Solid State Physics, University of Latvia, LV-1063 Riga, Latvia*

EPR spectra of $LiBaF_3$ crystals have been investigated after X-irradiation at RT. A spectrum consisting of approximately 35 nearly equidistant EPR lines has a strong angular dependence on the line intensities. The spectrum is caused by a hyperfine interaction (hfs) of a spin $S = 1/2$ with neighbouring groups of nuclei. The observed large number of hfs lines required Li nuclei being in the first shell and fluorine nuclei in the more distant second shell. We analysed the spectrum in the *F*-centre model, taking reduced hfs values of the *F*-centre in LiF and found qualitative explanation of the number of hfs lines. The angular dependence of the line intensities could be explained by an anisotropy of the *g*-tensor with its main axis along the [1 0 0] axis of the crystal.

*Keywords*: Electron paramagnetic resonance; Radiation defects; $LiBaF_3$ crystals

## 1. INTRODUCTION

$LiBaF_3$ is a promising crystal for various applications as scintillator [1] and dosimeter, however, the structure of the radiation defects needs further investigations. EPR of several iron group impurities [2] and the $Ce^{3+}$ impurity [3] have been reported. After X-irradiation at low temperatures, EPR spectra of the self-trapped hole centres $V_K(F_2^-)$ have been observed [4]. After X-irradiation at room temperature (RT), several absorption bands of radiation defects have been observed and analysed in terms of *F*-type centres and their aggregates [5, 6], no EPR spectra of these defects have been identified.

The aim of the present work was to investigate the hyperfine structure (hfs) of the EPR spectra of the $LiBaF_3$ crystals after X-irradiation at RT.

## 2. EXPERIMENTAL RESULTS

Figure 1 shows EPR spectra of a nominally non-doped $LiBaF_3$ (curve a) and of a Fe-doped $LiBaF_3$ (curve b) crystals after X-irradiation at RT. Several EPR line groups could be observed. As a rule, intense EPR lines around $g = 2$ are always present, however they differ in different nominally non-doped samples. The strong central line in the Fe-doped crystal could partially contain EPR lines of $Fe^{3+}$.

* Corresponding author. E-mail: rogulis@labnet.lv

ISSN 1042-0150 print; ISSN 1029-4953 online 
DOI: 10.1080/1042015021000052971

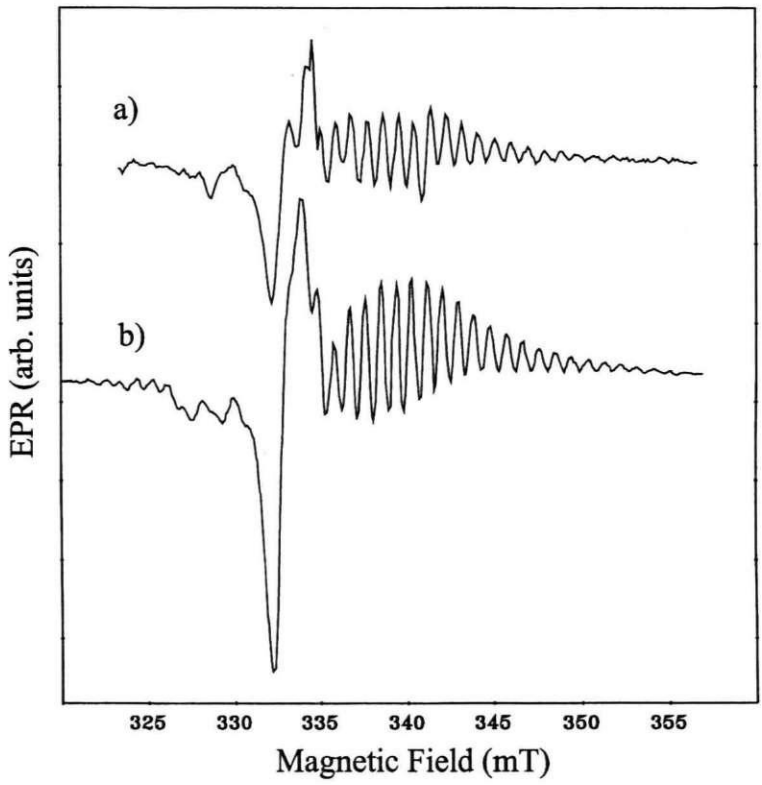


FIGURE 1 (a) EPR spectrum of (a) nominally non-doped $LiBaF_3$ crystal and (b) EPR spectrum of $LiBaF_3$:Fe crystal, X-irradiated and measured at RT for a magnetic field orientation B || [1 1 1]. The microwave frequency was 9.38 GHz.

A spectrum consisting of up to 35 nearly equidistant EPR lines on the high field site of the central lines could be observed in several nominally non-doped $LiBaF_3$ crystals. It is unstable at RT and disappeared within several hours in dark or even faster in light. This spectrum occurs not in all nominally non-doped samples, addition of impurities like Fe, In or Ni enhance the creation efficiency of this defect. Lines in the spectre are nearly equidistant and most intense at B || [1 1 1]. For all other orientation of the magnetic field the line intensities changed in a complicated way.

## 3. DISCUSSION

These EPR lines have been analysed as caused by a hyperfine interaction of an unpaired spin $S = 1/2$ with several equivalent neighbouring groups of nuclei. EPR spectrum has $g$-tensor values lower as for a free electron, therefore the defect could be attributed to an electron trap centre.

In the structure of $LiBaF_3$ shown in Figure 2, the lattice site of $F^-$, has two Li neighbours in the first shell and 8 fluorine in the second shell. The lattice site of $Li^+$ has 6 fluorine neighbours in the first shell and 8 barium neighbours in the second shell. The lattice site of $Ba^{2+}$ has 12 fluorine neighbours in the first shell and 8 lithium neighbours in the second shell.

We found, that taking into account only fluorine neighbours in the first and second shells, it is not possible to explain the large number of lines in our EPR spectrum.

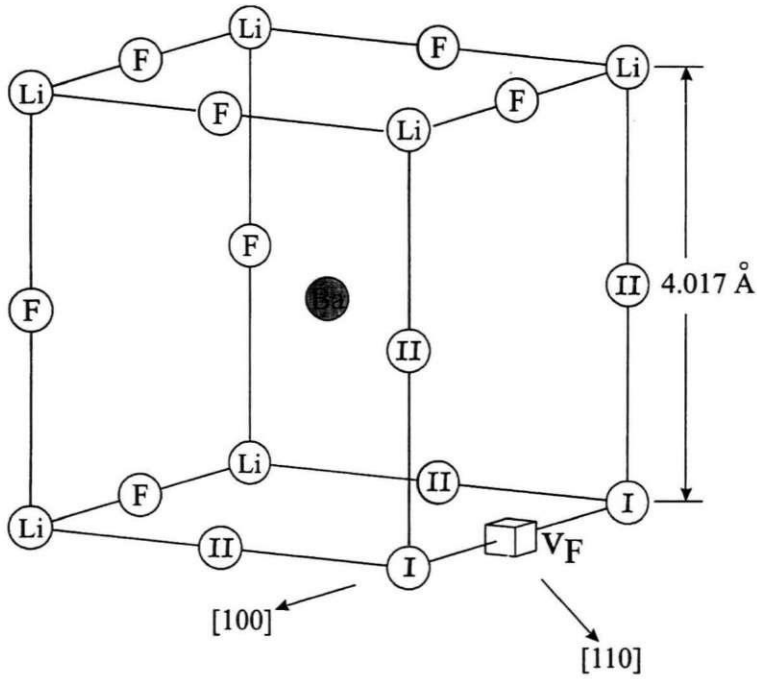


FIGURE 2 Crystal structure of $LiBaF_3$ with *F*-centre. Fluorine vacancy has 2 Li neighbours (I) in the first shell and 8 fluorine neighbours (II) in the second shell.

To explain the observed large number of hfs lines, the interaction is required with Li nuclei in the first shell and fluorine nuclei being in the second shell. This order of shells takes place only for a fluorine lattice site in $LiBaF_3$ and leads to a *F*-like centre model, *i.e.* a fluorine vacancy with a trapped electron.

Fortunately, the lattice constant of $LiBaF_3$ ($a = 3.996$ Å) coincides well with the lattice constant of LiF ($a = 4.0173$ Å) and allows us to use as a first approximation the values of the hfs parameters found for the *F*-centre in neutron-irradiated LiF crystals [7]. We mentioned also some similarities between the spectra of the *F*-centre in LiF and our EPR spectrum. However, both the crystals have different numbers of lithium nuclei in the first neighbour shell of the fluorine vacancy (see Tab. I). For the *F*-centre in LiF, the first shell consists of 6 equivalent Li neighbours with smaller hfs values as the second, fluorine, shell with 8 equivalent neighbours. In $LiBaF_3$ crystal the fluorine site has 2 Li neighbours in the first shell and 8 neighbours in the second shell.

TABLE I Hyperfine Interaction Parameters of the EPR Spectrum for the *F*-centre in LiF [7] and Scaled Parameter Set Used in the Present Work for the *F*-centre Model in $LiBaF_3$. We Assumed for $LiBaF_3$ the Same Ratio Between the *a* and *b* Parameters as in LiF.

| | *Nuclei data* | | | *LiF [7]* | | | *$LiBaF_3$* | | |
|---|---|---|---|---|---|---|---|---|---|
| *Shells* | *Isotope* | *Spin* | *(%)* | *Nuclei* | *a (mT)* | *b (mT)* | *Nuclei* | *a (mT)* | *b (mT)* |
| I | $Li^7$ | 3/2 | 92.5 | 6 | 1.394 | 0.114 | 2 | 0.91 | 0.07 |
| | $Li^6$ | 1 | 7.5 | | 0.528 | 0.043 | | 0.34 | 0.03 |
| II | $F^{19}$ | 1/2 | 100 | 8 | 3.780 | 0.534 | 8 | 3.20 | 0.45 |

Applying the hfs parameter values from the *F*-centre in LiF, we could not reproduce the spectrum well in Figure 1b for the B ‖ [1 1 1]. Taking reduced Li hfs parameters of about 35% and reduced fluorine shell hfs parameters of about 15% (listed in Tab. I), we found qualitatively good explanation of the number of hfs lines and reproduce at least qualitatively the EPR spectrum for the B ‖ [1 1 1] direction (Fig. 3b).

The strong angular dependence of the line intensities (not shown) could be explained by an anisotropy of the *g*-tensor with its main axis oriented along the [1 0 0] axis of the crystal.

Preliminary analysis of the EPR spectra in the magnetic field directions B ‖ [1 0 0] and B ‖ [1 1 0] gave a following estimation for the main values of the *g*-tensor: $g_{\parallel} = 2.00$ and $g_{\perp} = 1.96$. These values could be corrected by more detailed calculations of the angular dependence of the spectra.

In conclusion, we found a strong evidence, that the observed EPR spectrum with up to 35 hfs lines in X-irradiated samples belongs to the *F*-centre in $LiBaF_3$.

Further calculations are needed to determine precisely the set of the hfs and *g*-tensor parameters. Substitution in the first Li shell or in the second-fluorine shell should lead to significant reduction of the number of the hfs lines but we could not exclude the possible perturbation in the EPR spectrum in the third shell or further neighbour shells.

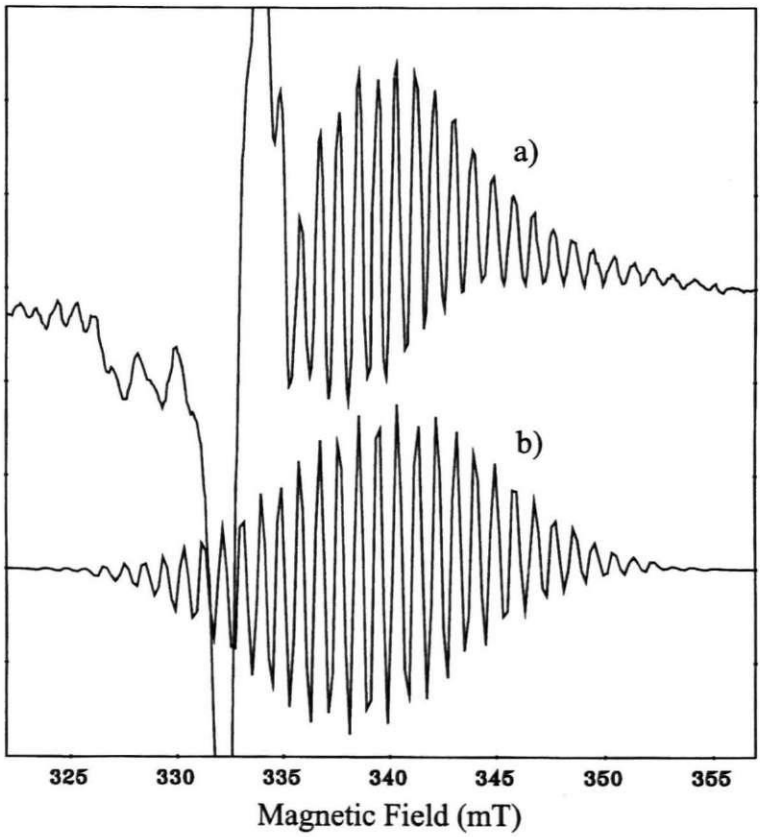


FIGURE 3 (a) EPR spectrum of $LiBaF_3$:Fe crystal, *x*-irradiated and measured at RT for a magnetic field orientation B ‖ [1 1 1]. (b) Calculated EPR spectrum for a magnetic field orientation B ‖ [1 1 1] with parameters of Table I.

## *References*

[1] van Eijk, C. W. E. (2001). *Nucl. Instr. and Meth.*, **460**, 1.
[2] Yosida, T., Aoki, H., Takeuchi, H., Arakawa, M. and Horai, K. (1979). *J. Phys. Soc. Japan, Letters*, **46**, 1661.
[3] Yamaga, M., Honda, M., Shimamura, K., Fukuda, T. and Yosida, T. (2000). *J. Phys.: Condens. Matter*, **12**, 5917.
[4] Tale, I., Springis, M., Rogulis, U., Ogorodnik, V., Kulis, P., Tale, V., Veispals, A. and Fitting, H.-J. (2001). *Rad. Eff. and Def. in Solids*, **155**, 51.
[5] Prado, L., Gomes, L., Baldochi, S. L., Morato, S. P. and Vieira, N. D., Jr. (1998). *J. Phys.: Condens. Matter*, **10**, 8247.
[6] Tale, I., Kulis, P., Rogulis, U., Tale, V., Trokss, J., Veispals, A., Barboza-Flores, M. and Fitting, H.-J. (1997). *J. Luminescence*, **72–74**, 722.
[7] Kaplan, R. and Bray, P. J. (1963). *Phys. Rev.*, **129**, 1919.

LATVIAN JOURNAL OF PHYSICS AND TECHNICAL SCIENCES
2004, N 2

*SOLID STATE PHYSICS*

# EPR OF F-TYPE CENTRES IN $LiBaF_3$

V. Ogorodnik, U. Rogulis,
I. Tale, A. Veispals

Institute of Solid State Physics, University of Latvia
Ķengaraga iela 8, LV-1063, Riga, LATVIA

In the present work, we have investigated in more detail the EPR spectrum of defects observed in $LiBaF_3$ crystals after X-irradiation at room temperature, consisting of approximately 35 lines. Such a defect is unstable at RT and disappears within few hours in the dark and even faster in the light. These EPR lines are equidistant (with a step of 0.9 mT) for the orientation of magnetic field parallel to the <111> direction of the crystal, with their intensities closely obeying a binomial distribution. The spectrum has been explained by hyperfine interaction (*hf*) of a spin S = ½ with two equivalent Li nuclei that are in the first shell and eight equivalent fluorine nuclei in the second shell. This model corresponds to the F-type centre (a fluoride vacancy with an electron) in $LiBaF_3$ crystal. The strong angular dependence of the line intensities is caused by an anisotropy of the *g*-tensor whose main axis is oriented along the [100] direction of the crystal. In the work, angular dependences of the *hf* lines and their intensities as well as possible parameters of the *g*-tensor are discussed.

## 1. INTRODUCTION

$LiBaF_3$ crystals are interesting for applications as scintillators, storage prosphors or dosimeters, and detectors of the slow neutron particles [1]. After X-irradiation of $LiBaF_3$ at room temperature (RT), several optical absorption bands of radiation defects have been observed and analysed in terms of F-type centres and their aggregates [2, 3]. EPR data on iron group impurities and $Ce^{3+}$ impurity are reported in [4] and [5], respectively. After X-irradiation at low temperatures, EPR spectra of the self-trapped hole centres – $V_K(F_2^-)$ – were identified [6]. In our previous work [7] we reported preliminary results on the EPR spectrum of a radiation defect created by X-irradiation at RT. It is unstable at RT and disappears within few hours in the dark and faster in the light. The spectrum, consisting of up to 35 hyperfine structure (*hf*) lines with a strong angular dependence of the line intensities, was tentatively ascribed to an F-type centre (an electron trapped on a fluorine vacancy). In the present work we are proceeding further with the analysis of complicated EPR line intensity variations at the angles other than B ll [111] and provide a further estimation of the EPR *hf* parameters as well as a rough estimate of the *g*-tensor elements.

## 2. EXPERIMENTAL

$LiBaF_3$ crystal doped with 0.1 % Fe (grown at the Institute of Solid State Physics, University of Latvia, Riga), and oriented by X-ray diffraction (at the Institute of Physics, Czech Academy of Sciences, Prague), in order to allow rotation of the magnetic field in the (110) plane. The sample was X-irradiated at RT, kept in the dark, and measured by an X-band (9 GHz) EPR spectrometer within few hours after the irradiation.

## 3. RESULTS AND DISCUSSION

Figure 1 shows experimental EPR spectra of $LiBaF_3$ crystal, X-irradiated at RT and asured at different orientations of the magnetic field in the (110) plane. The intense tral line at about 333 mT is not discussed in the present work. We will consider here a of *hf* lines in the magnetic field range of up to 355 mT.

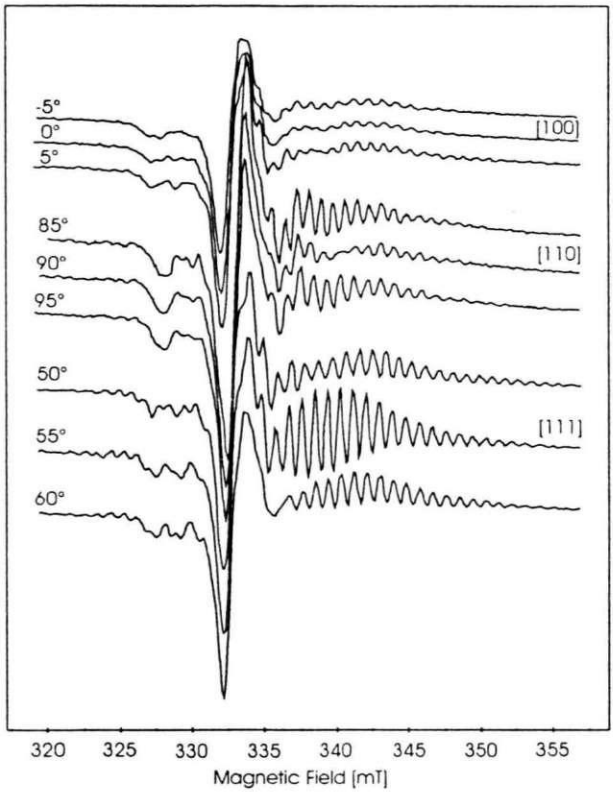


*Fig. 1.* EPR spectra of $LiBaF_3$:Fe crystal, X-irradiated and measured at RT for a magnetic field orientation along the main axis of the crystal. The values on the left of the curves are the angle of magnetic field and the [100] axis in the (110) plane. The microwave frequency was 9.38 GHz

The EPR spectrum is simplified at the orientation of the magnetic field B ll [111] l in this orientation it has nearly binomial distribution of the line intensities. For the B ll 0] orientation of magnetic field the line intensity decreases and the spectrum seems to be ided into two groups. At the B ll [100] orientation the line intensity sharply decreases. e angular dependence of EPR line intensities in Fig. 1 is very strong, and the angle iations of 5° can change the spectra completely. Therefore we will analyse the spectra y for three definite magnetic field orientations along the main crystal axes of the $LiBaF_3$.

We have analysed EPR spectra for all the three orientations with the spin Hamil-ian:

$$\hat{H} = \mu_B \vec{B} \bar{\bar{g}} \vec{\bar{S}} + \sum_{i=1}^{8} \vec{\bar{S}} \hat{\bar{A}}_i \vec{\bar{I}}_F + \sum_{j=1}^{2} \vec{\bar{S}} \hat{\bar{A}}_j \vec{\bar{I}}_{Li} , \qquad (1)$$

ere $g$ and $\hat{A}_i$ $\hat{A}_j$ are the $g$-tensor and *hf* tensors, respectively, and $\mu_B$ is the Bohr gneton.

Analysis of spectra in the F-type centre model, assuming reduced *hf* values of the F-ıtre in LiF crystals [8], allowed a qualitative explanation of the number of *hf* lines [7] for

the B ll [111] orientation. The spectrum is explained by a hyperfine interaction of the spin $S = ½$ with two equivalent Li nuclei being in the first shell (I) and eight equivalent fluorine nuclei in the second shell (II) (see Fig. 2).

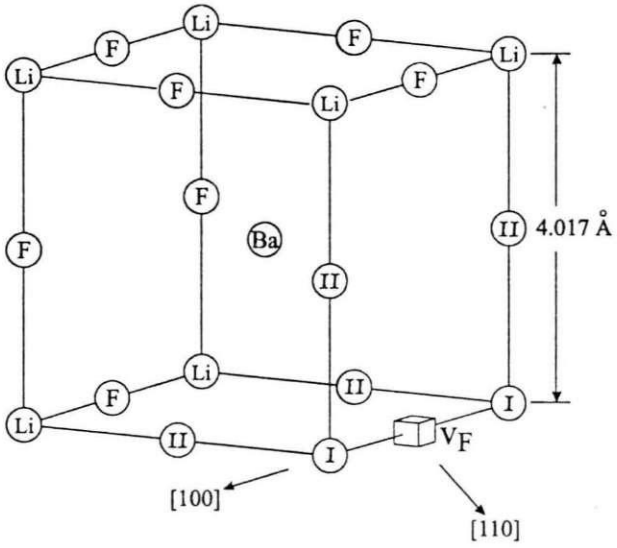


*Fig. 2.* Crystal structure of $LiBaF_3$ with F-type centre. Fluorine vacancy has two Li neighbours (I) in the first shell and eight fluorine neighbours (II) in the second shell

According to this model – with an unpaired spin localised in the fluorine vacancy – we set the main axes of the hyperfine interaction tensors for fluorine nuclei in [110] directions and for lithium nuclei – in [100] directions.

In the present work, we have corrected the preliminary *hf* parameter values (taken from [7]) in order to explain, at least qualitatively, the orientations other than Bll [111] of the EPR spectrum. The corrected *hf* parameters are shown in Table 1. These (*hf*) parameters have a usual meaning, i.e. $\mathbf{A_\perp = a-b}$ , $\mathbf{A_{||} = a+2b}$.

*Table 1*

**Spin Hamiltonian parameters of the EPR spectrum for the F-type centre in $LiBaF_3$. Hyperfine interaction parameters are given in mT**

| a ($F^{19}$) | b ($F^{19}$) | a ($Li^7$) | b ($Li^7$) | $g_{||}$ | $g_\perp$ |
|---|---|---|---|---|---|
| 3.12 | 0.20 | 0.91 | 0.03 | 1.990 | 1.960 |
| ±0.02 | ±0.02 | ±0.02 | ±0.01 | ±0.005 | ±0.005 |

Figure 3 shows experimental spectra (curves *a*) and simulated spectra (curves *b*), respectively, for the B ll [111] orientation of the magnetic field. It is seen that there is a good quantitative coincidence of the line positions and a qualitative coincidence of the line intensities. In our previous report [7] we already suggested that the *g*-tensor of our F-type centre could be aligned along the [100] direction of $LiBaF_3$ crystal. In the present work, we are proceeding with more detailed analysis of the EPR spectra, for the orientation of magnetic field along the [100] and [110] axes of the crystal. With the parameters shown in Table 1, it was possible to qualitatively explain the spectrum division into two groups at the B ll [110] orientation (Fig. 4, curve *b*). At the Bll[100] orientation the line intensity in the experimental spectrum is low and it has neither the binomial distribution nor it is divided into groups (Fig. 5, curve *a*). The simulated spectrum in Fig. 5 (curve *b*) also has a lower

ɛnsity than in other orientations. This could be explained by an "interference" of two *hf* ɛ groups with different *g*-values for two non-equivalent centre orientations at B ll [100].

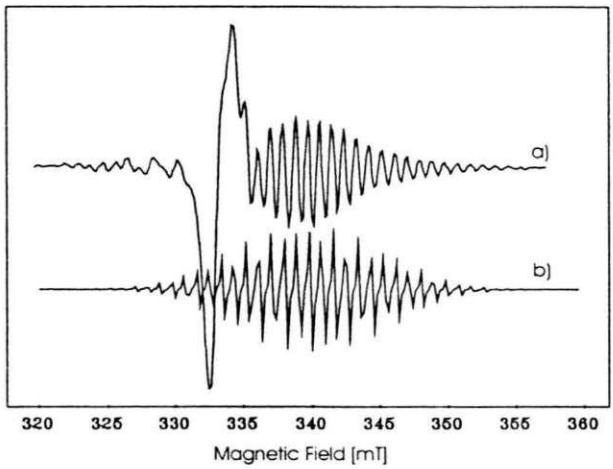


*Fig. 3.* (*a*) EPR spectrum of $LiBaF_3$:Fe crystal, X-irradiated and measured at RT for B ll [111] magnetic field orientation; (*b*) calculated EPR spectrum for B ll [111] magnetic field orientation with parameters of Table 1

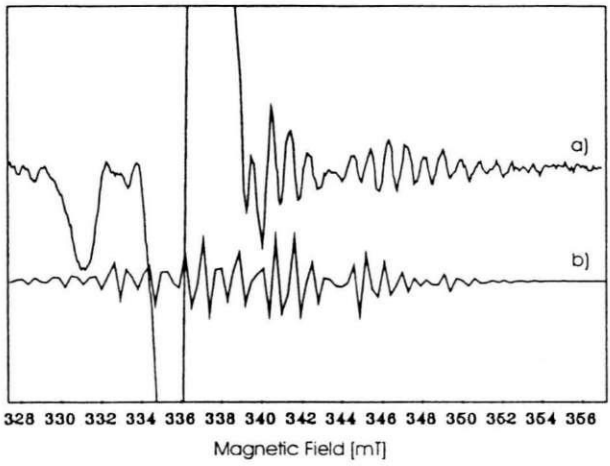


*Fig. 4.* (*a*) measured and (*b*) calculated EPR spectrum for B ll [110]

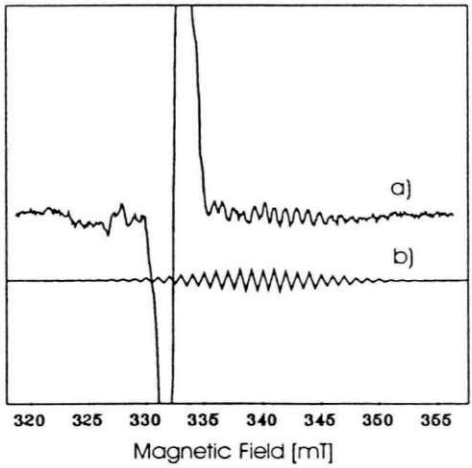


*Fig. 5.* (*a*) measured and (*b*) calculated EPR spectrum for B ll [100]

Therefore, for B ll [100] and B ll [110] orientations the spectra could be satisfactorily explained by a $g$-tensor of axial symmetry with its main axis aligned along the [100] direction. The estimated $g$-tensor values are $g_{||}$=1,99 and $g_{\perp}$=1,96 (see Table 1). Other alignments of the main axes of $g$-tensors contradict with the observed angular dependences of the line intensities, particularly with the number of groups of the *hf* lines at different orientations. The $g$–tensor anisotropy changes the position of EPR lines for each of the *hf* groups. At different orientations the overlapping of both the *hf* groups causes the total intensity variations of the whole spectra at different magnetic field orientations.

## 4. CONCLUSION

Our present analysis corroborates the model of F-type centres in $LiBaF_3$. However, a slight perturbation in the third and/or farther co-ordination spheres, which are not of significant influence for *hf* lines, should not be excluded. Finally, in the present work we have analysed, qualitatively and quantitatively, the angular dependence of EPR line intensity of the F-type centre in $LiBaF_3$ crystal, based on the set of *hf*- and $g$-tensor parameters obtained. However, the code used by us did not allow the spectra to be calculated for all possible magnetic field orientations. To do this, a more complicated code is needed. Further investigations are also necessary in order to find out correlation with the optical properties of F-type centres.

## REFERENCES


1. Knitel M.J., Dorenbos P., de Haas J.T.M., van Eijk C. W. E. (1996) $LiBaF_3$ a thermal neutron scintillator with optimal n-gamma discrimination *Nucl. Instr. and Meth. A* **374** 197–201.
2. Kulis P., Tale I., Springis M., Rogulis U., Trokss J., Veispals A., Fitting H.-J. (1999) F-type centres in $LiBaF_3$ crystals *Rad. Effects and Defects in Solids* **149** 97–100.
3. Prado L., Gomes L., Baldochi S.L., Morato S.P., Vieira Jr.N.D. (1998) Electron-irradiation-induced defects in $LiBaF_3$ crystals *J. Phys.: Condens. Matter.* **10** 8247–8256.
4. Yosida T., Aoki H., Takeuchi H., Arakawa M., Horai K. (1979) EPR of several iron-group impurities in $LiBaF_3$ having inverse perovskite structure *J. Phys. Soc. Japan Letters* **46** 1661–1662.
5. Yamaga M., Honda M., Shimamura K., Fukuda T., Yosida T. (2000) Electron spin-resonance study on $Ce^{3+}$ in $BaLiF_3$ *J. Phys. Condens. Matter* **12** 5917-5928.
6. Tale I., Springis M., Rogulis U., Ogorodnik V., Kulis P., Tale V., Veispals A., Fitting H.-J. (2001) Self-trapped holes in $LiBaF_3$ crystals *Rad. Efects and Defects in Solids* **155** 51–54.
7. Rogulis U., Ogorodnik V., Tale I., Veispals A. (2002) EPR of radiation defects in $LiBaF_3$ crystals *Rad. Effects and Defects in Solids* **157** 699–703.
8. Kaplan R., Bray P.J. (1963) Electron-Spin Paramagnetic Resonance Studies of Neutron-Irradiated LiF *Phys. Rev. b* **129** 1919–1935.

# F-TIPA CENTRU EPR $LiBaF_3$

V. Ogorodniks, U. Rogulis, I. Tale, A. Veispals

Kopsavilkums

Izpētīts ar rentgenu istabas temperatūrā apstarotā $LiBaF_3$ kristālā radīta defekta EPR spektrs. EPR spektrs sastāv no apmēram 35 ekvidistantām līnijām. Defekts ir nestabils dienas gaismā, bet tumsā sabrūk dažu stundu laikā. Šīs līnijas magnētiskā lauka orientācijā paralēli [111] kristāla asij atrodas vienādos attālumos (ar soli 0,9 mT) ar intensitāšu sadalījumu tuvu binomiālajam. EPR spektru var aprakstīt kā nesapārota spina S = 1/2 hipersīkstruktūras (*hss*) mijiedarbību ar divām ekvivalentu kaimiņu kodolu spinu grupām: 2 Li kodoliem pirmajā grupā un 8 F kodoliem otrajā grupā. Šāds modelis atbilst F-tipa centram (elektrons atrodas fluora vakancē) $LiBaF_3$ kristālā. Līniju intensitāšu stipro leņķisko atkarību nosaka *g*-tenzors ar tā galveno asi virzītu [100] virzienā. Darbā analizētas *hss* līniju leņķiskās atkarības un iespējamie *g*-tenzora parametri.

12.03.2004.